

Primary production in the Southern Ocean, 1997–2006

Kevin R. Arrigo,¹ Gert L. van Dijken,¹ and Seth Bushinsky¹

Received 11 September 2007; revised 24 April 2008; accepted 19 May 2008; published 5 August 2008.

[1] Estimates of primary production in the Southern Ocean are difficult to obtain but are essential if we are to understand its role in the global carbon cycle. Here we present a 9-year time series of daily primary production calculated from remotely sensed ocean color, sea surface temperature, and sea ice concentration using a primary production algorithm parameterized specifically for use in Southern Ocean waters. Results suggest that total annual production in waters south of 50°S averaged $1949 \pm 70.1 \text{ Tg C a}^{-1}$ (where a is years) between 1998 and 2006, approximately half that of previous estimates. The large but relatively unproductive pelagic province accounted for ~90% of Southern Ocean production, while area normalized rates of production were greatest on the much smaller continental shelf ($109 \text{ g C m}^{-2} \text{ a}^{-1}$). Surprisingly, production in the marginal ice zone was only slightly higher than in the pelagic province. The Ross Sea was the most productive sector of the Southern Ocean (mean = 503 Tg C a^{-1}), followed closely by the Weddell Sea (mean = 477 Tg C a^{-1}). Unlike the Arctic Ocean, there was no secular trend in either sea ice cover or annual primary production in the Southern Ocean during our 9-year study. Interannual variability in annual production was most closely tied to changes in sea ice cover, although changes in sea surface temperature also played a role. Only 31% of the variation in annual production was explained by the Southern Annular Mode. Annual primary production could increase in the future as stronger winds increase nutrient upwelling.

Citation: Arrigo, K. R., G. L. van Dijken, and S. Bushinsky (2008), Primary production in the Southern Ocean, 1997–2006, *J. Geophys. Res.*, 113, C08004, doi:10.1029/2007JC004551.

1. Introduction

[2] The polar Southern Ocean (waters south of 50°S) is a critical component of global ocean circulation and the biogeochemical cycles of nutrients and carbon. Despite the fact that it represents only 10% of total ocean surface area, it accounts for approximately 25% of the oceanic uptake of atmospheric CO₂ [Takahashi *et al.*, 2002]. Much of this CO₂ sink has been attributed to cooling of southward flowing subtropical surface waters and the associated increase in CO₂ solubility (i.e., the solubility pump). Some of the highest concentrations and deepest penetration of anthropogenic carbon are found in the Southern Ocean [Lo Monaco *et al.*, 2005; Waugh *et al.*, 2006], particularly in the northward moving Antarctic Bottom Water [Sabine *et al.*, 2002]. Because these bottom waters were recently in contact with the atmosphere, they are an important water mass for the storage of anthropogenic CO₂ in the deep ocean [McNeil *et al.*, 2001].

[3] Another key mechanism that facilitates the influx of atmospheric CO₂ into the Southern Ocean is the biological pump, whereby phytoplankton photosynthesis reduces the surface water partial pressure of CO₂ (pCO₂), creating a

gradient between the ocean and atmosphere. When this newly fixed organic carbon sinks out of the upper mixed layer, it may be stored within the deep ocean circulation system for hundreds of years [Broecker, 1991]. Hence, Southern Ocean regions with high rates of phytoplankton primary production and an active biological pump are important sites mediating the ocean-atmosphere exchange of CO₂.

[4] On average, the Southern Ocean is characterized by its abundant macronutrients coupled with only modest rates of annual average net primary production [Arrigo *et al.*, 1998a; Moore and Abbott, 2000]. Despite the generally low phytoplankton abundance, intense phytoplankton blooms occasionally develop, making productivity in the Southern Ocean highly variable both temporally and spatially. The lowest rates of production are generally associated with pelagic waters north of the sea ice zone (SIZ), where rates range from 0.08 to $0.22 \text{ g C m}^{-2} \text{ d}^{-1}$ in June to $0.5\text{--}1.0 \text{ g C m}^{-2} \text{ d}^{-1}$ in December [Arrigo *et al.*, 1998a]. Low production rates in these waters are the result of a variety of factors, including low sun angles, deep mixing of the upper water column, and trace metal limitation [Martin, 1990; Mitchell and Holm-Hansen, 1991; Boyd *et al.*, 2000]. One exception to the usually low rates of production characterizing waters north of the SIZ are found along oceanographic fronts, such as the Antarctic Polar Front, where divergence of surface waters brings waters with high nutrient concentrations to the surface, fueling enhanced phytoplankton growth [Moore

¹Department of Environmental Earth System Science, Stanford University, Stanford, California, USA.

and Abbott, 2000; Hense et al., 2000]. Another exception is found near offshore islands (e.g., the Balleny Islands and South Georgia Island), where current flow past rough or shallowing topography also can increase the flux of nutrients into surface waters [Korb and Whitehouse, 2004].

[5] The highest rates of primary production in the Southern Ocean are generally associated with coastal polynyas (regions of open water surrounded by sea ice) [Arrigo and Van Dijken, 2003, 2007], the marginal ice zone (MIZ) [Smith and Nelson, 1986], and the continental shelf [Smith and Gordon, 1997; Sweeney, 2003; Arrigo and Van Dijken, 2004]. In these environments, rates of CO₂ fixation frequently exceed 2 g C m⁻² d⁻¹, sufficient to maintain a positive CO₂ gradient between the ocean surface and the atmosphere, facilitating the influx of atmospheric CO₂ [e.g., Louanchi et al., 1999a, 1999b; Sweeney, 2003].

[6] Much of what is currently known about large-scale patterns in primary productivity of the Southern Ocean comes from a small number of studies using either satellite-based methods [Arrigo et al., 1998a; Moore and Abbott, 2000; Gabric et al., 2002; Lovenduski and Gruber, 2005; Carr et al., 2006] or numerical models [Fennel et al., 2003; Sarmiento et al., 2004]. However, for a variety of different reasons, these studies have been limited in their ability to assess the spatial variability in Southern Ocean primary production over both short (weekly) and long (interannual) timescales. Here we present an analysis of a nearly decade-long time series of primary productivity determined from space-based measurements of sea ice distribution, sea surface temperature, and chlorophyll *a* (Chl *a*) concentration, together with estimates of mixed layer depth, cloud cover, and spectral irradiance. The algorithm used here to estimate depth-integrated primary productivity is a modified version of that presented by Arrigo et al. [1998a]. The current algorithm has been more rigorously validated and benefits from the far superior spatial and temporal Chl *a* coverage afforded by the Sea-viewing Wide Field of view Sensor compared to the Coastal Zone Color Scanner (CZCS). The primary goal of this study was to quantify spatial variability and interannual changes in primary production within the Southern Ocean and relate the observed patterns to concurrent variability in environmental forcing and climate state (e.g., the Southern Annular Mode (SAM)).

2. Methods

2.1. Primary Production Algorithm

[7] The algorithm (modified from Arrigo et al. [1998a]) calculates the rate of primary production (mg C m⁻³ hr⁻¹) as a function of diurnal changes in spectral downwelling irradiance, sea surface temperature (°C), and Chl *a* concentration (mg m⁻³). Horizontal distributions of Chl *a* were determined from 8-day mean Sea-viewing Wide Field-of-view Sensor (SeaWiFS) imagery (9 km resolution) for the period 1997–2006. We assume that Chl *a* concentration is uniform within the upper mixed layer and decreases exponentially at greater depths, according to the relationship

$$\text{Chl } a(z) = \text{Chl } a(0) \exp[0.033(z - \text{MLD})], \quad (1)$$

where *z* is depth, Chl *a*(0) is the surface Chl *a* concentration determined from SeaWiFS data, and MLD is the depth of

the mixed layer, determined using the model of Markus [1999]. This relationship was determined using a large number of vertical Chl *a* profiles from the Southern Ocean [Arrigo et al., 2000]. Because waters below the mixed layer account for a small fraction of depth-integrated primary production, the algorithm is relatively insensitive to this parameterization. Primary productivity at each SeaWiFS pixel location is integrated over depth (0–100 m at 1 m intervals) and time (hourly for 24 h) to determine daily primary production (mg C m⁻² d⁻¹).

[8] The radiative transfer model of Gregg and Carder [1990] is used to compute clear sky downwelling irradiance (*E*_{clear}) at hour *t* which is subsequently corrected for fractional cloud cover (*N*) according to the equation of Dobson and Smith [1988]

$$E_d(\lambda, t) = E_{\text{clear}}(\lambda, t)[1 - 0.53(N^{0.5})], \quad (2)$$

where *E*_d is the cloud corrected downwelling irradiance, λ is wavelength (nm) and values for *N* are based on NCEP/NCAR daily reanalysis data [Kalnay et al., 1996]. Other inputs to the radiative transfer model (sea level pressure, wind speed, precipitable water, air temperature, and specific humidity) are also from the NCEP/NCAR Reanalysis project, except for ozone (NASA's Total Ozone Mapping Spectrometer project).

[9] Irradiance is propagated through the water column according to the equation

$$E_d(\lambda, z, t) = (1 - R)E_d(\lambda, t) \exp[-K_d(\lambda)z], \quad (3)$$

where *z* is depth (m), and *R* is the surface reflection [McClain et al., 1996] and

$$K_d(\lambda) = \frac{a_w(\lambda) + a_d(\lambda) + a_s(\lambda) + a_{ph}^*(\lambda) \text{Chl } a + b_{bw}(\lambda) + b_{bp}(\lambda)}{\mu}, \quad (4)$$

where μ is the mean cosine of the angular irradiance distribution, *a* is absorption, *a**_{ph} is the Chl-*a*-specific absorption by phytoplankton from Arrigo et al. [1998b], and *b*_b is backscatter. The subscripts *w* and *p* represent contributions by seawater and particles, respectively. The inherent optical properties *a*_w, *b*_{bw}, and *b*_{bp} are obtained from Pope and Fry [1997] and Smith and Baker [1981]. Using data from the Ross Sea [Arrigo et al., 1998b], detrital absorption is assumed to vary spectrally and as a function of Chl *a* concentration according to the equation

$$a_d(\lambda) = 0.006 \text{ Chl } a \exp(-0.0143(\lambda - 400)) \quad (5)$$

and soluble absorption by CDOM is estimated by

$$a_s(\lambda) = 0.025 \exp(-0.012(\lambda - 400)). \quad (6)$$

Daily primary production (*PP*, mg C m⁻² d⁻¹) integrated over the upper 100 m is calculated as

$$PP = \int_{z=0}^{100} \int_{t=0}^{24} \text{Chla}(z) \frac{C}{\text{Chla}} G(z, t) dt dz, \quad (7)$$

where $\text{Chl } a(z)$ is the Chl a concentration at depth z , $C/\text{Chl } a$ is the phytoplankton carbon to Chl a ratio (88.5 g:g), and $G(z, t)$ is the net biomass-specific growth rate (h^{-1}) at a given time t and depth z .

[10] G is calculated as a product of the temperature-dependent upper limit to net phytoplankton growth rate, G_{\max} (h^{-1}) and the irradiance limitation term, L (dimensionless), such that

$$G(z, t) = G_{\max}(t)L(z, t). \quad (8)$$

$G_{\max}(t)$ is calculated according to the equation

$$G_{\max}(t) = G_o \exp[rT(t)], \quad (9)$$

where G_o is the phytoplankton net growth rate at 0°C (0.59 day^{-1}) and r is a rate constant ($0.0633^\circ\text{C}^{-1}$) that determines the sensitivity of G_{\max} to temperature, T ($^\circ\text{C}$) [Eppley, 1972]. The sea surface temperature at time t is obtained from version 2 of the NOAA optimum interpolation sea surface temperature, OISST V2 [Reynolds et al., 2002], and assumed to be constant with depth. While not strictly true, depth-dependent variability in T in the upper ocean tends to be small in polar waters so the impact of this assumption is relatively minor.

[11] The light limitation term, $L(z, t)$, is calculated for each depth and each time step as

$$L(z, t) = 1 - \exp\left(-\frac{\text{PUR}(z, t)}{E_k'(z, t)}\right), \quad (10)$$

where $\text{PUR}(z, t)$ is the photosynthetically usable radiation and $E_k'(z, t)$ is the spectral photoacclimation parameter [Arrigo and Sullivan, 1994]. Both $\text{PUR}(z, t)$ and $E_k'(z, t)$ are in units of $\mu\text{Ein m}^{-2} \text{ s}^{-1}$. Phytoplankton growth is effectively light saturated when $\text{PUR} \approx 3E_k'$. PUR is a function of the spectral irradiance and phytoplankton spectral absorption [Morel, 1978]

$$\text{PUR}(z, t) = \int_{\lambda=400}^{700} E_d(\lambda, z, t) \frac{a^*(\lambda)}{a_{\max}^*} d\lambda, \quad (11)$$

where a_{\max}^* is the maximum value attained by the phytoplankton absorption coefficient, $a^*(\lambda)$, and $E_d(\lambda, z, t)$ is the spectral downwelling irradiance at depth z and time t . $\text{PUR}(z, t)$ is used to calculate PUR^* , a measure of the average amount of usable radiation available during the photoperiod, F , according to the equations: if $z \leq \text{MLD}$,

$$\text{PUR}^*(z) = \frac{\int_{z=0}^{\text{MLD}} \int_{t=12-F/2}^{12+F/2} \text{PUR}(z, t) dt}{F \text{MLD}} \quad (12a)$$

and if $z > \text{MLD}$,

$$\text{PUR}^*(z) = \frac{\int_{t=12-F/2}^{12+F/2} \text{PUR}(z, t) dt}{F}. \quad (12b)$$

In this way, PUR^* represents a value averaged both over the photoperiod and over depth within the mixed layer (i.e., PUR^* will be uniform with depth within the mixed layer), while below the mixed layer, PUR^* represents a value averaged only over the photoperiod (i.e., PUR^* will vary with depth below the mixed layer).

[12] $E_k'(z, t)$ in equation (10) varies as a function of PUR^* according to the equations [Arrigo and Sullivan, 1994]

$$E_k'(z) = \frac{E_k'^{\max}}{1 + 2 \exp[-B \text{PUR}^*(z)]} \quad (13)$$

$$B = \exp[1.089 - 2.12 \log(E_k'^{\max})], \quad (14)$$

where $E_k'^{\max}$ is the maximum observed value for E_k' . Arrigo et al. [1998a] compiled spectral irradiance data and corresponding values of E_k' for phytoplankton collected over a wide range of times, depths, and locations in the Southern Ocean and determined that $E_k'^{\max} \approx 80 \mu\text{Ein m}^{-2} \text{ s}^{-1}$. Equations (13) and (14) scale $E_k'(z)$ with depth to simulate photoacclimation such that $E_k'(z)$ asymptotically approaches $E_k'^{\max}$ and $E_k'^{\min}$ ($= 26.4 \mu\text{Ein m}^{-2} \text{ s}^{-1}$ as defined in equation (13)) toward the surface and base of the euphotic zone, respectively.

2.2. Defining Regions of Interest

[13] For the purpose of this study, the Southern Ocean (defined as the area south of 50°S) is divided into five geographic sectors (Figure 1) and four ecological provinces (Figure 2). Geographic sectors are defined simply by longitude and include the Weddell Sea (60°W – 20°E), south Indian Ocean (20 – 90°E), southwestern Pacific Ocean (90 – 160°E), Ross Sea (160°E – 130°W), and Bellingshausen-Amundsen Sea (130 – 60°W). The four ecological provinces (Figure 2) are defined on the basis of sea ice coverage and bathymetry and include the pelagic, the MIZ, the continental shelf, and the MIZ-shelf (that part of the MIZ on the continental shelf). Their size is quantified over time by the amount of open water in each (i.e., the size of the shelf province is smaller in the winter than in the summer because it is mostly ice covered during the winter).

[14] Sea ice extent used to define boundaries of ecological provinces is determined from Special Sensor Microwave Imager (SSM/I) data using the PSSM algorithm of Markus and Burns [1995]. In this approach, the boundary between sea ice and open water is approximately the 10% sea ice concentration contour. The pelagic province is defined as waters south of 50°S that have been ice free for >14 days and where water depth is >1000 m. South of the pelagic province is the SIZ which contains the MIZ, the shelf, and the MIZ-shelf provinces. The shelf province is defined as waters with a depth of <1000 m that have been ice free for >14 days. The MIZ province is associated with the retreating sea ice edge and is defined operationally as any open water pixel where sea ice was present some time in the last 14 days. Anywhere that the MIZ extends onto the shelf is considered part of the MIZ-shelf province. Once a given MIZ or MIZ-shelf pixel has been ice free longer than the 14-day threshold, it is redefined as being part of the pelagic or shelf province, respectively, depending on water depth. Because of the high temporal variability in the extent

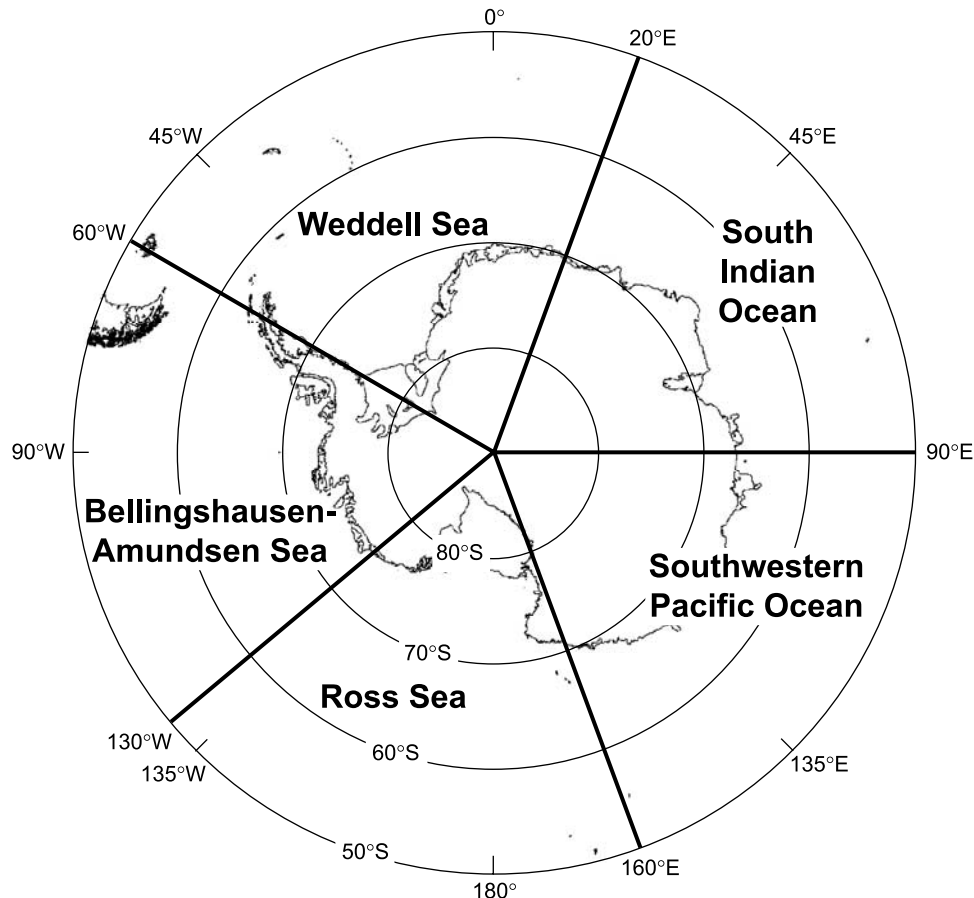


Figure 1. Map of the study area showing the location of the five geographic sectors.

of the sea ice cover, the size of all ecological provinces varies daily. The portions of the Patagonian and New Zealand shelves which extend south of 50°S are excluded from all analyses to avoid confusion with productivity on the Antarctic continental shelf.

[15] The threshold for the MIZ of 14 days was calculated from observations of the horizontal distance the surface meltwater layer extended perpendicularly from the ice edge and the number of days taken for sea ice to retreat that distance. On the basis of three well-documented MIZs, we calculate that low salinity surface waters persist for approximately 14 days after the sea ice has retreated from a given region. After that time, advection and mixing by winds have weakened surface stratification and the phytoplankton bloom collapses. For example, satellite imagery of sea ice extent shows that the ice edge in the Weddell Sea where *Smith and Nelson* [1986] conducted their study was retreating at a rate of 8.3 km d^{-1} (250 km of ice retreat in 30 days). Given that the far edge of the phytoplankton bloom was located 170 km from the ice edge, this suggests that the MIZ persisted for 20 days ($170 \text{ km}/8.3 \text{ km d}^{-1} = 20 \text{ days}$). *Lancelot et al.* [1991] transected the ice edge three times during their study in the spring of 1988. Between their 26–30 November and 20–24 December transects, the ice edge had retreated 160 km, or 6.4 km d^{-1} . The far side of the phytoplankton bloom was 100 km from the ice edge, implying a MIZ persistence time of 15 days. Between the 20–24 December and 27–31 December transect, ice edge

retreat had accelerated to a rate of 14 km d^{-1} (100 km in 7 days), resulting in a MIZ persistence time of 10 days (the far side of the phytoplankton bloom was 140 km from the ice edge; $140 \text{ km}/14 \text{ km d}^{-1} = 10 \text{ days}$). On the basis of these three values (20, 15, and 10 days), we chose the value of two weeks as a reasonable length of time a pixel should be considered as part of the MIZ.

[16] The primary productivity algorithm is forced with daily input, with the exception of SeaWiFS Chl *a* and OISST, which are 8-day means to reduce data gaps due to cloud cover. All model input fields are mapped to a common grid and each pixel is assigned to the appropriate geographic sector (e.g., Weddell Sea and Ross Sea) and ecological province (e.g., pelagic, MIZ, and shelf).

3. Algorithm Validation

3.1. Chlorophyll *a*

[17] The primary productivity algorithm presented here was validated in two steps and consisted of the evaluation of SeaWiFS Chl *a* retrievals using the OC4v4 algorithm [*O'Reilly et al.*, 1998] and comparisons of Chl-*a*-based primary production obtained in situ with those computed by our primary productivity algorithm. Previous efforts to validate SeaWiFS Chl *a* in the Southern Ocean have met with decidedly mixed results. *Barbini et al.* [2006] reported that in the southwestern Ross Sea, the SeaWiFS OC4v4 algorithm overestimated Chl *a* at high concentrations and

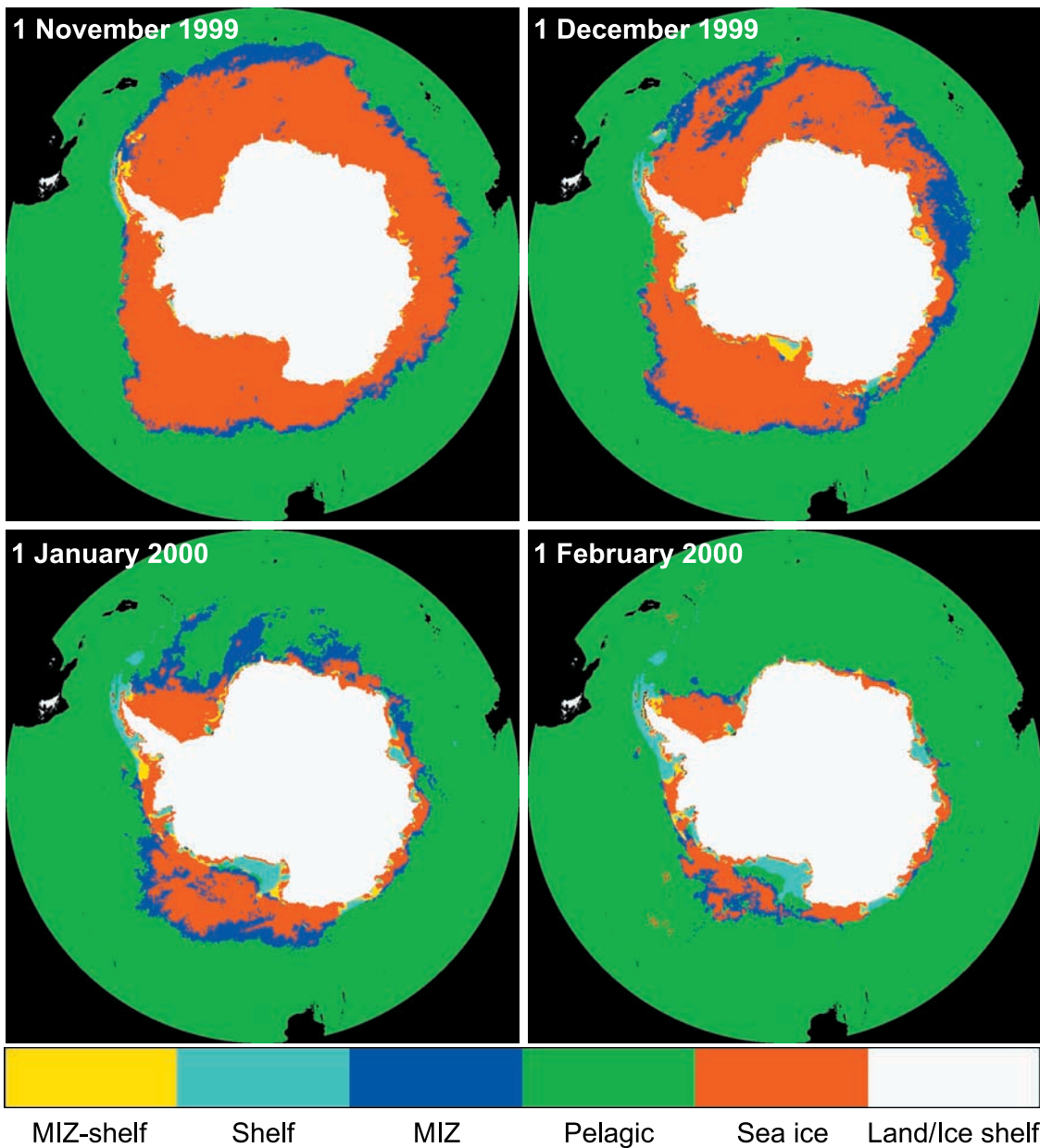


Figure 2. Maps showing how the four ecological provinces (pelagic, MIZ, shelf, and MIZ-shelf) used in the present study vary in size and location over time during the major phytoplankton growing season.

underestimated them at low concentrations. This is the reverse of what is found in the CCAMLR region of the WAP [Holm-Hansen *et al.*, 2004], where SeaWiFS slightly overestimated Chl *a* at concentrations below $0.2 \text{ mg Chl } a \text{ m}^{-3}$ and underestimated in situ values at higher Chl *a* concentrations. Garcia *et al.* [2005] reported similar underestimates by the OC4v4 algorithm, particularly at concentrations above $0.2 \text{ mg Chl } a \text{ m}^{-3}$ for the nearby Bransfield Strait region, with an overall Southern Ocean bias of -21.7% . Korb *et al.* [2004] calculated that in waters around South Georgia Island in the Scotia Sea, SeaWiFS underestimated Chl *a* by only 15% at concentrations below $1 \text{ mg Chl } a \text{ m}^{-3}$ but this underestimate increased to 70% at Chl *a* concentrations above $5 \text{ mg Chl } a \text{ m}^{-3}$.

[18] However, a recent analysis by Marrari *et al.* [2006], also for the western Antarctic Peninsula, showed that if in situ Chl *a* is determined using high performance liquid chromatography (HPLC), rather than fluorometry, the differences between SeaWiFS-derived Chl *a* and in situ Chl *a* virtually disappear. Similarly, Arrigo and Van Dijken [2004] used HPLC-derived Chl *a* data from the Ross Sea to show that over a Chl *a* range of $0.2\text{--}10 \text{ mg m}^{-3}$, the SeaWiFS OC4v4 algorithm is within 10% of in situ values.

[19] Because these validation exercises covered such a limited area of the Southern Ocean, we conducted a larger-scale Chl *a* comparison, similar to that performed earlier by Sullivan *et al.* [1993] for the CZCS. In evaluating SeaWiFS Chl *a* estimates, 5854 in situ surface Chl *a* samples were obtained from the NASA SeaBASS bio-optical data archive

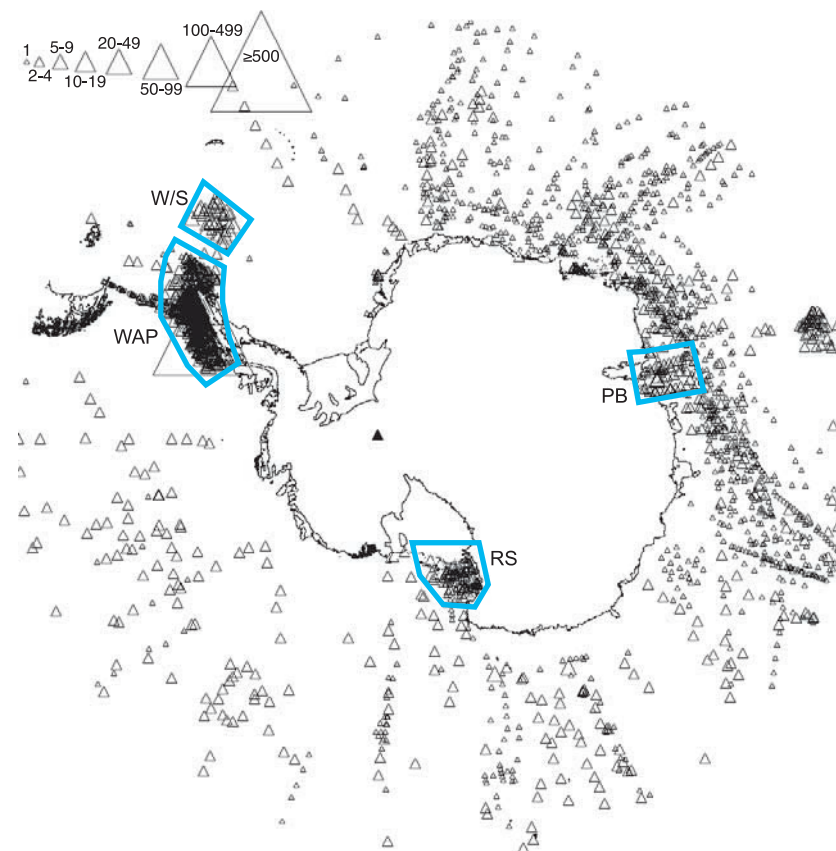


Figure 3. Locations in the Southern Ocean where Chl *a* samples used to validate the SeaWiFS OC4v4 algorithm were collected. The number of samples in a given location is given by the size of the triangles. Separate analyses were carried out for each of the delineated regions. W/S, Weddell/Scotia Sea; RS, Ross Sea; PB, Prydz Bay; WAP, Western Antarctic Peninsula.

and compared to Chl *a* estimates derived from SeaWiFS for corresponding regions and time periods. This particular analysis is complicated by three factors, (1) the Southern Ocean in situ Chl *a* data set from SeaBASS is heavily biased toward high Chl *a* waters, (2) the data set consists mostly of fluorometrically derived Chl *a*, and (3) most in situ data were obtained before 1997, precluding their direct comparison with SeaWiFS-derived Chl *a*. Nevertheless, we were interested in confirming that the frequency distribution of Chl *a* for the Southern Ocean determined using SeaWiFS is consistent with that generated from in situ data.

[20] The bias toward high Chl *a* concentrations in the in situ data set is a consequence of the historically high sampling effort in productive regions such as the Ross Sea continental shelf, the Weddell/Scotia Sea, Prydz Bay, and most notably, the WAP, where a single station has been sampled >500 times (Figure 3). To reduce this high Chl *a* bias as much as possible, we divided the Southern Ocean into five different geographic regions, each of which is analyzed separately. These five regions included the Ross Sea continental shelf, the WAP, the Weddell/Scotia Sea, Prydz Bay, and the “oceanic” Southern Ocean, which consists largely of low Chl *a* waters north of the Antarctic continental shelf.

[21] For all Southern Ocean waters south of 50°S, in situ and SeaWiFS estimates of Chl *a* averaged 0.54 and 0.34 mg Chl *a* m⁻³, respectively (Table 1). Although both data sets

exhibited a maximum number of samples in the 0.10–0.15 mg Chl *a* m⁻³ range, there are substantially more in situ samples with values above 0.20 mg Chl *a* m⁻³ (Figure 4a). Many of these high Chl *a* samples were collected in the WAP, which exhibited a relatively large difference between in situ and SeaWiFS-derived Chl *a* (Table 1 and Figure 4b, note the isolated peak at 2.3 mg Chl *a* m⁻³ here and in Figure 4a). As shown in Figure 3, most of the in situ samples from the WAP were collected in coastal waters while the SeaWiFS analysis included more offshore areas. This disparity resulted in the mean Chl *a* concentration for the in situ WAP data (1.91 mg Chl *a* m⁻³) being almost fourfold higher than the SeaWiFS-derived estimates for the same region (0.53 mg Chl *a* m⁻³).

Table 1. Mean Chlorophyll *a* in the Southern Ocean Derived In Situ and Using SeaWiFS^a

	SeaWiFS	In Situ
Southern Ocean	0.34	0.54
Southern Ocean (offshore waters only)	0.28	0.36
West Antarctic Peninsula (WAP)	0.53	1.91
Ross Sea	2.18	2.53
Weddell/Scotia Sea	0.62	0.92
Weddell/Scotia Sea (minus Scotia Ridge)	0.62	0.61
Prydz Bay	1.06	0.92

^aMean chlorophyll *a* given in mg m⁻³.

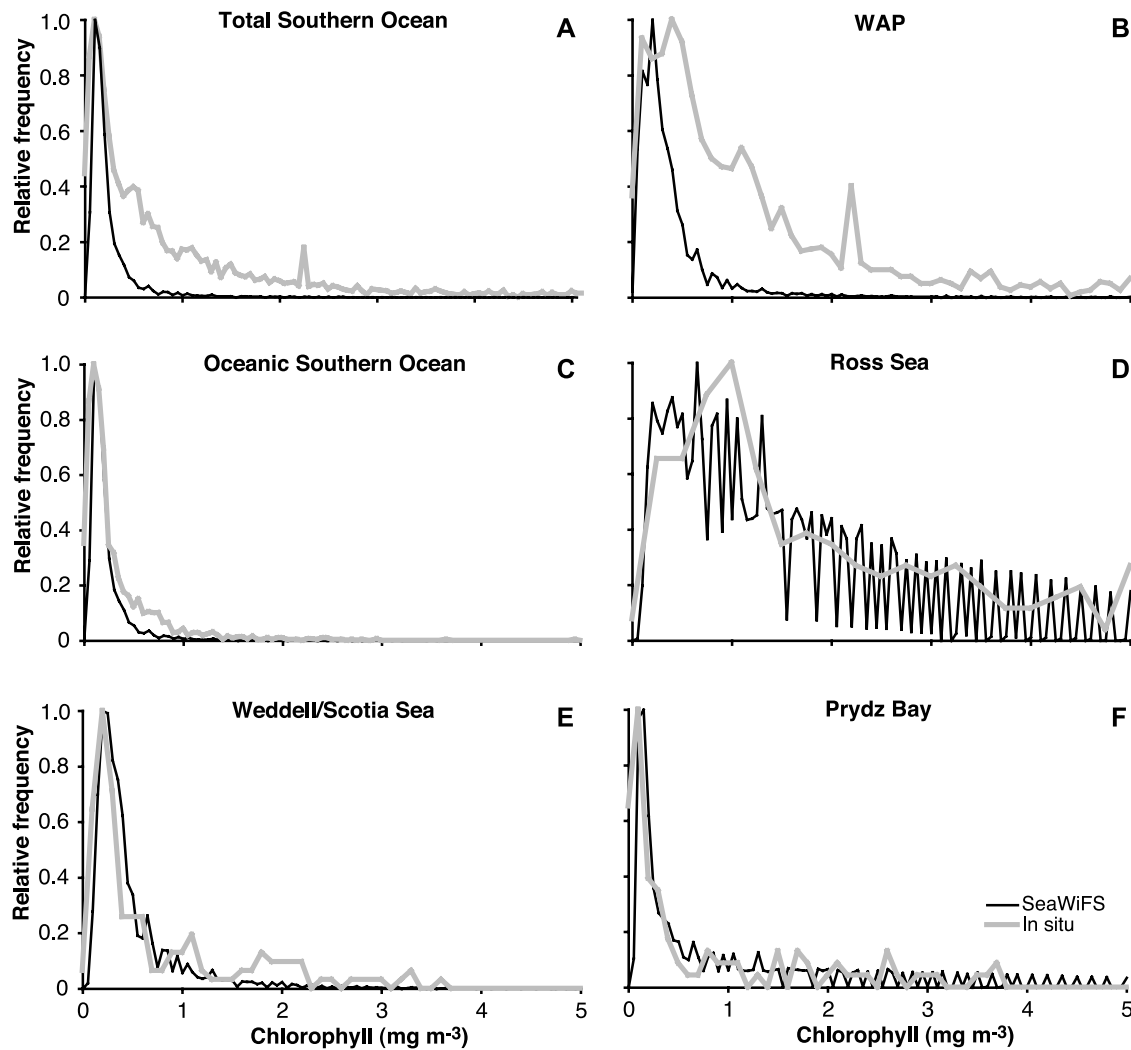


Figure 4. Relative frequency distributions for Chl *a* measured in situ and from SeaWiFS for (a) all waters south of 50°S, (b) the Western Antarctic Peninsula (WAP), (c) deep waters of the Southern Ocean, (d) the Ross Sea, (e) the Weddell/Scotia Sea, and (f) Prydz Bay. The boundaries of each region are given in Figure 3.

[22] When the high productivity regions of the Southern Ocean are excluded from the analysis, the frequency distributions for Chl *a* determined from in situ and from SeaWiFS data are in much better agreement (Figure 4c), averaging 0.36 mg Chl *a* m⁻³ and 0.28 mg Chl *a* m⁻³, respectively. As discussed earlier, much of the remaining difference is likely attributable to the fact that the historical in situ Chl *a* was determined primarily using fluorometric methods, which overestimate Chl *a* relative to the HPLC method [Marrari *et al.*, 2006]. Similarly, frequency plots of in situ Chl *a* for the Ross Sea (Figure 4d), Weddell/Scotia Sea (Figure 4e), and Prydz Bay (Figure 4f) are in good agreement with similar plots made from SeaWiFS-derived Chl *a*. These three regions have much more widespread and uniform in situ data coverage than the WAP (Figure 3) and are less heavily biased toward higher coastal values. Although the frequency plots are similar, the mean in situ Chl *a* for the Weddell/Scotia Sea (0.92 mg Chl *a* m⁻³) is about 50% higher than the SeaWiFS-derived value (0.62 mg Chl *a* m⁻³).

This is due to the large number of samples collected near the Scotia Ridge and South Georgia Island (Figure 3). When these high Chl *a* samples are excluded, the in situ mean drops to 0.61 mg Chl *a* m⁻³, in much better agreement with SeaWiFS data (Table 1).

[23] Consequently, on the basis of our own and previous analyses of SeaWiFS Chl *a* in the Southern Ocean, we conclude that the SeaWiFS OC4v4 algorithm performs adequately when compared to in situ Chl *a*, assuming that Chl *a* is determined using HPLC, and when the in situ data set is adjusted to account for its bias toward high values. Therefore, we elected to use the standard SeaWiFS OC4v4 Chl *a* values as input to the primary productivity algorithm.

3.2. Primary Productivity

[24] Ideally, the primary production algorithm used here would be validated by comparing its output for a specific day and location to measurements made in situ at the same time and location. Unfortunately, because of the high degree

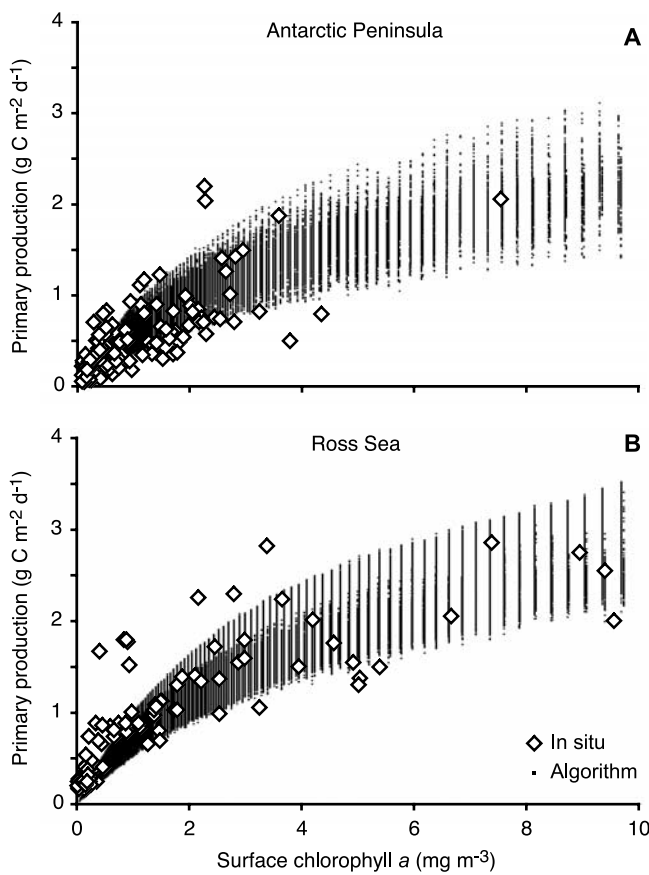


Figure 5. Plots of primary production versus Chl *a* derived by the primary production algorithm and measured in situ at discrete stations (a) near the Antarctic Peninsula ($64\text{--}73^{\circ}\text{W}$, $64\text{--}68^{\circ}\text{S}$) and (b) in the Ross Sea ($165^{\circ}\text{E}\text{--}165^{\circ}\text{W}$, $74\text{--}78^{\circ}\text{S}$). Algorithm output used in this analysis was restricted to those times and locations for which in situ data were available.

of phytoplankton patchiness, the large amount of cloud cover in the Southern Ocean, and the relatively few direct field observations collected since 1997, there are too few coincident satellite-derived and in situ estimates of production to perform a statistically valid comparison. Instead, we opted to validate our algorithm by first assuming that the SeaWiFS surface Chl *a* retrievals are reliable and then comparing regressions of primary production against surface Chl *a* produced by our algorithm to similar regressions generated using in situ Chl *a* and primary production data from the Ross Sea ($165^{\circ}\text{E}\text{--}165^{\circ}\text{W}$, $74\text{--}78^{\circ}\text{S}$) and the Antarctic Peninsula ($64\text{--}73^{\circ}\text{W}$, $64\text{--}68^{\circ}\text{S}$). These two locations were chosen because both have ample data from which to derive a statistically significant relationship between Chl *a* and daily primary production and because the dynamic range in both Chl *a* and primary production is large enough to represent the range of variability characteristic of the Southern Ocean.

[25] In the in situ primary productivity database for the Antarctic Peninsula, surface Chl *a* ranged from 0.10 to 14.64 mg m^{-3} and primary production from 42.5 to $2466 \text{ mg C m}^{-2} \text{ d}^{-1}$ ($n = 134$). The regression of in situ

primary production against in situ Chl *a* for the Antarctic Peninsula is remarkably similar to a corresponding plot made by regressing SeaWiFS retrievals of Chl *a* against primary production calculated from our primary productivity algorithm for the same geographical region and time period (Figure 5a). Both exhibit similar shapes and slopes and the range of primary productivity values computed for a given Chl *a* concentration is similar in both data sets. This range in algorithm-derived primary production for a given Chl *a* concentration is due to the fact that regions with similar surface Chl *a* concentration are still likely to differ in their solar zenith angle, cloud cover, mixed layer depth, and sea surface temperature and thus will yield different estimates of daily primary productivity.

[26] In the Ross Sea data set, in situ Chl *a* ranges from 0.03 to 14.56 mg m^{-3} while the corresponding measurements of primary production range from 156.1 to $2847 \text{ mg C m}^{-2} \text{ d}^{-1}$ ($n = 95$). Again, there is a very good correspondence between the in situ- and algorithm-derived regressions of daily primary production against surface Chl *a* (Figure 5b). Whereas the Antarctic Peninsula data set has a high proportion of observations at Chl *a* concentrations below 2 mg m^{-3} , the Ross Sea has substantially more observations at higher levels of phytoplankton biomass, making it a more appropriate test for high productivity regions of the Southern Ocean. These results suggest that, to the extent that Chl *a* retrievals from SeaWiFS are accurate, the primary productivity algorithm used here produces results that are fully consistent with in situ observations of primary production.

4. Results

4.1. Open Water Area

4.1.1. All Southern Ocean Waters

[27] The extent of open water area in the Southern Ocean over an annual cycle varies slightly from year to year between 1997 and 2006, averaging $34.14 \pm 0.23 \times 10^6 \text{ km}^2$ (Table 2). Open water area exhibits a distinct seasonal cycle (Figure 6a), increasing rapidly in size from its early spring minimum ($27.5 \times 10^6 \text{ km}^2$) to its peak in early March ($42.5 \times 10^6 \text{ km}^2$). There is no significant temporal trend with time between 1997 and 2006 in the amount of annual mean open water area in the Southern Ocean (Table 3).

4.1.2. Pelagic Province

[28] The pelagic province is by far the largest of the four open water ecological provinces in the Southern Ocean, averaging $32.0 \pm 0.19 \times 10^6 \text{ km}^2$ over an annual cycle (Figure 6b) and accounting for an average of 94% of total open water area south of 50°S (Table 2). When considered over the entire Southern Ocean, the pelagic province exhibits the smallest amount of interannual variability of the four ecological provinces (Figure 6b), with the coefficient of variation ($\text{CV} = 100 \bullet \text{standard deviation}/\text{mean}$) of only 0.6% (Table 2). Surprisingly, the proportion of total Southern Ocean area covered by the pelagic province is largest in the winter, despite a much higher sea ice cover in the Southern Ocean during that season. This is because open water in the pelagic province covers a relatively large area of at least $\sim 25 \times 10^6 \text{ km}^2$ in late winter/early spring (Figure 6b) while the other ecological provinces remain either small (because of a trivial amount of sea ice retreat in

Table 2. Mean (Maximum) Open Water Area (10^6 km^2) by Geographic Sector and Ecological Province^a

	Pelagic	MIZ	Shelf	MIZ Shelf	Total
<i>Bellingshausen-Amundsen Sea</i>					
1997–1998	7.02 (7.73)	0.19 (0.84)	0.114 (0.35)	0.074 (0.25)	7.40 (8.28)
1998–1999	7.05 (7.77)	0.17 (0.63)	0.169 (0.45)	0.080 (0.21)	7.46 (8.41)
1999–2000	6.86 (7.67)	0.25 (0.79)	0.136 (0.37)	0.077 (0.20)	7.32 (8.39)
2000–2001	6.97 (7.70)	0.20 (0.69)	0.141 (0.33)	0.067 (0.19)	7.38 (8.22)
2001–2002	6.92 (7.77)	0.22 (0.95)	0.131 (0.34)	0.074 (0.21)	7.35 (8.37)
2002–2003	7.08 (7.89)	0.20 (0.68)	0.141 (0.45)	0.076 (0.20)	7.49 (8.45)
2003–2004	6.94 (7.74)	0.18 (0.57)	0.145 (0.41)	0.072 (0.18)	7.34 (8.34)
2004–2005	6.80 (7.74)	0.20 (0.64)	0.085 (0.23)	0.057 (0.22)	7.15 (8.24)
2005–2006	7.14 (7.83)	0.18 (0.60)	0.098 (0.26)	0.068 (0.20)	7.49 (8.25)
Mean	6.97 (7.76)	0.20 (0.71)	0.129 (0.35)	0.072 (0.21)	7.37 (8.33)
SD	0.11 (0.07)	0.02 (0.12)	0.026 (0.08)	0.007 (0.02)	0.11 (0.08)
<i>Ross Sea</i>					
1997–1998	6.91 (8.75)	0.30 (1.24)	0.060 (0.34)	0.052 (0.22)	7.32 (9.39)
1998–1999	6.43 (8.73)	0.39 (1.82)	0.096 (0.45)	0.041 (0.19)	6.96 (9.60)
1999–2000	6.62 (8.94)	0.38 (1.48)	0.102 (0.42)	0.042 (0.29)	7.14 (9.77)
2000–2001	6.71 (8.72)	0.31 (1.16)	0.068 (0.36)	0.046 (0.19)	7.13 (9.49)
2001–2002	6.81 (8.77)	0.41 (1.66)	0.099 (0.44)	0.042 (0.23)	7.36 (9.78)
2002–2003	6.91 (8.86)	0.30 (1.04)	0.021 (0.14)	0.041 (0.25)	7.27 (9.36)
2003–2004	7.00 (8.80)	0.34 (1.01)	0.055 (0.37)	0.050 (0.27)	7.44 (9.57)
2004–2005	6.99 (9.22)	0.34 (1.52)	0.103 (0.42)	0.040 (0.21)	7.48 (9.82)
2005–2006	6.98 (9.15)	0.35 (1.40)	0.105 (0.42)	0.045 (0.27)	7.48 (9.83)
Mean	6.82 (8.88)	0.35 (1.37)	0.079 (0.37)	0.044 (0.23)	7.29 (9.62)
SD	0.20 (0.19)	0.04 (0.28)	0.029 (0.10)	0.004 (0.04)	0.18 (0.18)
<i>South Indian Ocean</i>					
1997–1998	5.85 (7.52)	0.30 (1.65)	0.049 (0.20)	0.035 (0.13)	6.23 (7.80)
1998–1999	5.76 (7.52)	0.31 (1.58)	0.032 (0.15)	0.027 (0.09)	6.14 (7.77)
1999–2000	5.70 (7.45)	0.30 (1.22)	0.026 (0.14)	0.028 (0.09)	6.05 (7.72)
2000–2001	5.85 (7.55)	0.28 (1.45)	0.044 (0.18)	0.031 (0.09)	6.20 (7.80)
2001–2002	5.82 (7.43)	0.31 (1.46)	0.029 (0.15)	0.036 (0.10)	6.20 (7.71)
2002–2003	5.96 (7.56)	0.29 (1.34)	0.048 (0.19)	0.032 (0.08)	6.33 (7.82)
2003–2004	5.80 (7.56)	0.30 (1.38)	0.043 (0.19)	0.035 (0.09)	6.17 (7.83)
2004–2005	5.65 (7.50)	0.30 (1.48)	0.025 (0.11)	0.031 (0.15)	6.01 (7.74)
2005–2006	5.76 (7.57)	0.30 (1.60)	0.039 (0.18)	0.035 (0.12)	6.13 (7.82)
Mean	5.79 (7.52)	0.30 (1.46)	0.037 (0.16)	0.032 (0.10)	6.16 (7.78)
SD	0.09 (0.05)	0.01 (0.14)	0.010 (0.03)	0.003 (0.02)	0.10 (0.05)
<i>Southwest Pacific Ocean</i>					
1997–1998	6.23 (7.01)	0.22 (0.66)	0.033 (0.15)	0.040 (0.11)	6.52 (7.30)
1998–1999	6.10 (6.99)	0.23 (0.77)	0.033 (0.15)	0.039 (0.11)	6.40 (7.28)
1999–2000	6.14 (7.12)	0.23 (0.70)	0.054 (0.22)	0.047 (0.18)	6.47 (7.44)
2000–2001	6.27 (6.98)	0.22 (0.79)	0.026 (0.12)	0.039 (0.10)	6.55 (7.25)
2001–2002	6.35 (7.15)	0.21 (0.66)	0.057 (0.24)	0.058 (0.18)	6.68 (7.50)
2002–2003	6.31 (7.02)	0.19 (0.57)	0.037 (0.14)	0.042 (0.12)	6.58 (7.30)
2003–2004	6.19 (7.02)	0.25 (0.66)	0.034 (0.15)	0.043 (0.10)	6.51 (7.33)
2004–2005	6.28 (6.98)	0.22 (0.63)	0.035 (0.16)	0.046 (0.12)	6.58 (7.33)
2005–2006	6.21 (6.99)	0.21 (0.62)	0.032 (0.13)	0.039 (0.12)	6.49 (7.28)
Mean	6.23 (7.03)	0.22 (0.67)	0.038 (0.16)	0.044 (0.12)	6.53 (7.33)
SD	0.08 (0.06)	0.01 (0.07)	0.010 (0.04)	0.006 (0.03)	0.08 (0.08)
<i>Weddell Sea</i>					
1997–1998	6.06 (9.28)	0.46 (2.57)	0.131 (0.52)	0.067 (0.24)	6.72 (10.16)
1998–1999	6.52 (9.61)	0.42 (2.50)	0.113 (0.25)	0.048 (0.15)	7.10 (10.08)
1999–2000	6.47 (9.41)	0.41 (2.45)	0.115 (0.25)	0.047 (0.17)	7.04 (9.96)
2000–2001	6.10 (9.07)	0.41 (1.93)	0.092 (0.31)	0.061 (0.22)	6.66 (9.73)
2001–2002	6.38 (9.16)	0.48 (2.18)	0.144 (0.28)	0.045 (0.11)	7.05 (9.69)
2002–2003	5.77 (8.58)	0.40 (1.94)	0.095 (0.27)	0.069 (0.27)	6.34 (9.23)
2003–2004	5.88 (8.80)	0.49 (2.04)	0.092 (0.20)	0.045 (0.11)	6.50 (9.46)
2004–2005	6.24 (9.27)	0.45 (2.54)	0.117 (0.26)	0.052 (0.11)	6.85 (9.77)
2005–2006	6.19 (9.35)	0.46 (2.84)	0.109 (0.26)	0.061 (0.17)	6.81 (9.92)
Mean	6.18 (9.17)	0.44 (2.33)	0.112 (0.29)	0.055 (0.17)	6.79 (9.78)
SD	0.26 (0.32)	0.03 (0.32)	0.018 (0.09)	0.010 (0.06)	0.26 (0.30)
<i>Total</i>					
1997–1998	32.07 (40.13)	1.48 (4.88)	0.39 (1.46)	0.27 (0.74)	34.20 (42.75)
1998–1999	31.87 (40.56)	1.52 (5.93)	0.44 (1.42)	0.24 (0.53)	34.06 (43.05)
1999–2000	31.78 (40.30)	1.57 (5.09)	0.43 (1.36)	0.24 (0.64)	34.02 (43.12)
2000–2001	31.89 (39.97)	1.42 (4.57)	0.37 (1.24)	0.24 (0.62)	33.93 (42.24)
2001–2002	32.28 (40.10)	1.63 (5.54)	0.46 (1.42)	0.25 (0.64)	34.63 (42.91)
2002–2003	32.02 (39.67)	1.39 (4.59)	0.34 (1.06)	0.26 (0.72)	34.02 (41.89)
2003–2004	31.80 (39.86)	1.55 (4.98)	0.37 (1.24)	0.24 (0.63)	33.96 (42.35)
2004–2005	31.97 (40.66)	1.51 (5.57)	0.36 (1.13)	0.23 (0.58)	34.07 (42.71)
2005–2006	32.27 (40.84)	1.49 (5.52)	0.38 (1.15)	0.25 (0.62)	34.40 (42.93)
Mean	31.99 (40.23)	1.51 (5.19)	0.39 (1.28)	0.25 (0.64)	34.14 (42.66)
SD	0.19 (0.39)	0.07 (0.48)	0.04 (0.14)	0.01 (0.06)	0.23 (0.41)

^aMean (maximum) open water area given in 10^6 km^2 .

the MIZ and MIZ-shelf) or largely ice covered (e.g., shelf) during the winter. Seasonal changes in open water area are accompanied by a relatively small amount of high-frequency variability compared to the other provinces, particularly the MIZ and MIZ-shelf. This is due to the large size of the pelagic province and the fact that sea ice cover accounts for a much smaller fraction of total area in this province than it does in any of the other three provinces.

4.1.3. MIZ Province

[29] The MIZ is the second largest ecological province, covering an annual average of $1.51 \pm 0.07 \times 10^6 \text{ km}^2$ of the Southern Ocean between 1997 and 2006, and attaining a summer (December) maximum extent of $5.19 \pm 0.58 \times 10^6 \text{ km}^2$ (Table 2). The largest MIZ is found in the Weddell Sea sector, where it averages $0.44 \pm 0.03 \times 10^6 \text{ km}^2$ throughout the year, twice as large as the MIZ of the Southwest Pacific Ocean ($0.22 \pm 0.01 \times 10^6 \text{ km}^2$) and the Bellingshausen-Amundsen Sea ($0.20 \pm 0.02 \times 10^6 \text{ km}^2$) sectors. When averaged over an annual cycle, the size of the MIZ exhibits relatively little interannual variability, even when individual geographic sectors are considered (Table 2). However, shorter-term variation in the size of the MIZ can be quite large, particularly in the winter and spring (Figure 6c). In the most extreme case, the size of the MIZ in the Bellingshausen-Amundsen Sea can vary by as much as $0.6 \times 10^6 \text{ km}^2$ over weekly timescales; however short-term variability in the Ross Sea, the Southwest Pacific Ocean, and the Weddell Sea sectors is nearly as large.

4.1.4. Shelf Province

[30] The ice-free, non-MIZ, continental shelf is the next largest ecological province in the Southern Ocean, averaging $0.39 \pm 0.04 \times 10^6 \text{ km}^2$ in area over an annual cycle, with a peak summer open water area of $1.28 \pm 0.14 \times 10^6 \text{ km}^2$ (Figure 6d and Table 2). This province is largest in the Bellingshausen-Amundsen Sea (annual mean = $0.13 \pm 0.03 \times 10^6 \text{ km}^2$) and smallest in the South Indian Ocean and Southwest Pacific Ocean sectors, where its mean annual extent is only $0.04 \pm 0.01 \times 10^6 \text{ km}^2$. Over the entire Southern Ocean, the CV of the mean annual open water area between 1997 and 2006 is $\sim 10\%$, much larger than that of any other ecological province (Table 2).

4.1.5. MIZ-Shelf Province

[31] Smallest of the four ecological provinces is the MIZ-shelf, averaging just $0.25 \pm 0.01 \times 10^6 \text{ km}^2$ over an annual cycle between 1997 and 2006, with a peak summertime area over the entire Southern Ocean averaging only $0.64 \times 10^6 \text{ km}^2$ (Figure 6e and Table 2). On average, the MIZ-shelf accounts for approximately 40% of total continental shelf area in the Southern Ocean. Like the MIZ, the size of the MIZ-shelf exhibits marked short-term variability. In addition, the amount of open water area associated with the MIZ-shelf exhibits a great deal of interannual variability with respect to both its magnitude and timing. Maximum open water area associated with the MIZ-shelf is the most variable in the Southwest Pacific Ocean sector, ranging from as low as $0.10 \times 10^6 \text{ km}^2$ in 2000–2001 and 2004–2005 to as high as $0.18 \times 10^6 \text{ km}^2$ in 1999–2000 and 2001–2002. Maximum open water area in this sector is usually reached in December or January, in contrast to the Bellingshausen-Amundsen Sea sector, where maximum open water area is not attained until February. In the Ross Sea and the Weddell Sea sectors, the size of the MIZ-shelf

usually peaks in December, but may be delayed until as late as February (e.g., 2002–2003). In the South Indian Ocean sector in 2004–2005 and 2005–2006, open water area in the MIZ-shelf did not reach its annual maximum until well into March.

4.2. Primary Productivity

4.2.1. All Southern Ocean Waters

[32] Like open water area, daily primary production in the Southern Ocean exhibits a distinct seasonal cycle, increasing exponentially from an average low of $\sim 60 \text{ mg C m}^{-2} \text{ d}^{-1}$ in August to an annual peak in December ranging from 325 to $425 \text{ mg C m}^{-2} \text{ d}^{-1}$, depending on the year (Figure 6f). Thereafter, daily primary production exhibits a consistent and rapid decline between January and March, dropping by 75% by the end of the austral summer. Over an annual cycle, daily primary production across the Southern Ocean averages $156 \text{ mg C m}^{-2} \text{ d}^{-1}$, or $57.0 \text{ g C m}^{-2} \text{ a}^{-1}$ (where a is years), (Table 4) between 1997 and 2006. The annual peak in primary production precedes the peak in open water area by 2–3 months. Given that the seasonal decline in primary production begins in early summer (January), prior to refreezing of the ice pack or the autumn increase in wind speeds (and associated vertical mixing and decreased irradiance), the dramatic drop in productivity is most likely attributable to inadequate nutrient supplies, most likely iron [Arrigo et al., 2000; Gervais et al., 2002; Coale et al., 2004], although an increase in grazer populations cannot be discounted. Not surprisingly, interannual variability in primary production is greatest during the spring and summer, when daily rates of production are highest (Figure 6f).

[33] Total annual primary production in Southern Ocean waters south of 50°S averaged $1949 \pm 70.1 \text{ Tg C a}^{-1}$ during the 9 years of our study (Table 5). Interannual variability in total production is relatively small, with all years falling within 6% of the mean for the 1997–2006 time period. Productivity is greatest during 1999–2000 (2051 Tg C a^{-1}) and lowest the following year, in 2000–2001 (1830 Tg C a^{-1}), a difference of only 12%. In part, this small degree of interannual variability likely reflects the fact that both the annual mean ($33.9\text{--}34.6 \times 10^6 \text{ km}^2$) and maximum ($41.9\text{--}43.1 \times 10^6 \text{ km}^2$) open water area in the Southern Ocean vary by <2% between 1997 and 2006 (Table 2).

4.2.2. Pelagic Province

[34] Not surprisingly, the relatively low productivity of the Southern Ocean reflects the dominance of the large pelagic province, where over an annual cycle, daily productivity averages only $148 \text{ mg C m}^{-2} \text{ d}^{-1}$ (Table 4) ranging seasonally from 50 to $70 \text{ mg C m}^{-2} \text{ d}^{-1}$ in the austral winter to $300\text{--}400 \text{ mg C m}^{-2} \text{ d}^{-1}$ at the peak of the spring bloom (Figure 6g). Annual production in the pelagic province is greatest in the Ross Sea sector of the Southern Ocean, averaging $428 \pm 29.8 \text{ Tg C a}^{-1}$ between 1997 and 2006 (Table 5), followed closely by the Weddell Sea ($412 \pm 42.2 \text{ Tg C a}^{-1}$) and the Bellingshausen-Amundsen Sea ($357 \pm 14.5 \text{ Tg C a}^{-1}$) sectors.

[35] Approximately 90% of total annual primary production in the Southern Ocean between 1997 and 2006 is associated with the pelagic province (annual mean = $1729 \pm 60.7 \text{ Tg C a}^{-1}$), due principally to its large size relative to the other ecological provinces, but also to its longer-ice-free phytoplankton growing season. This proportion is attribut-

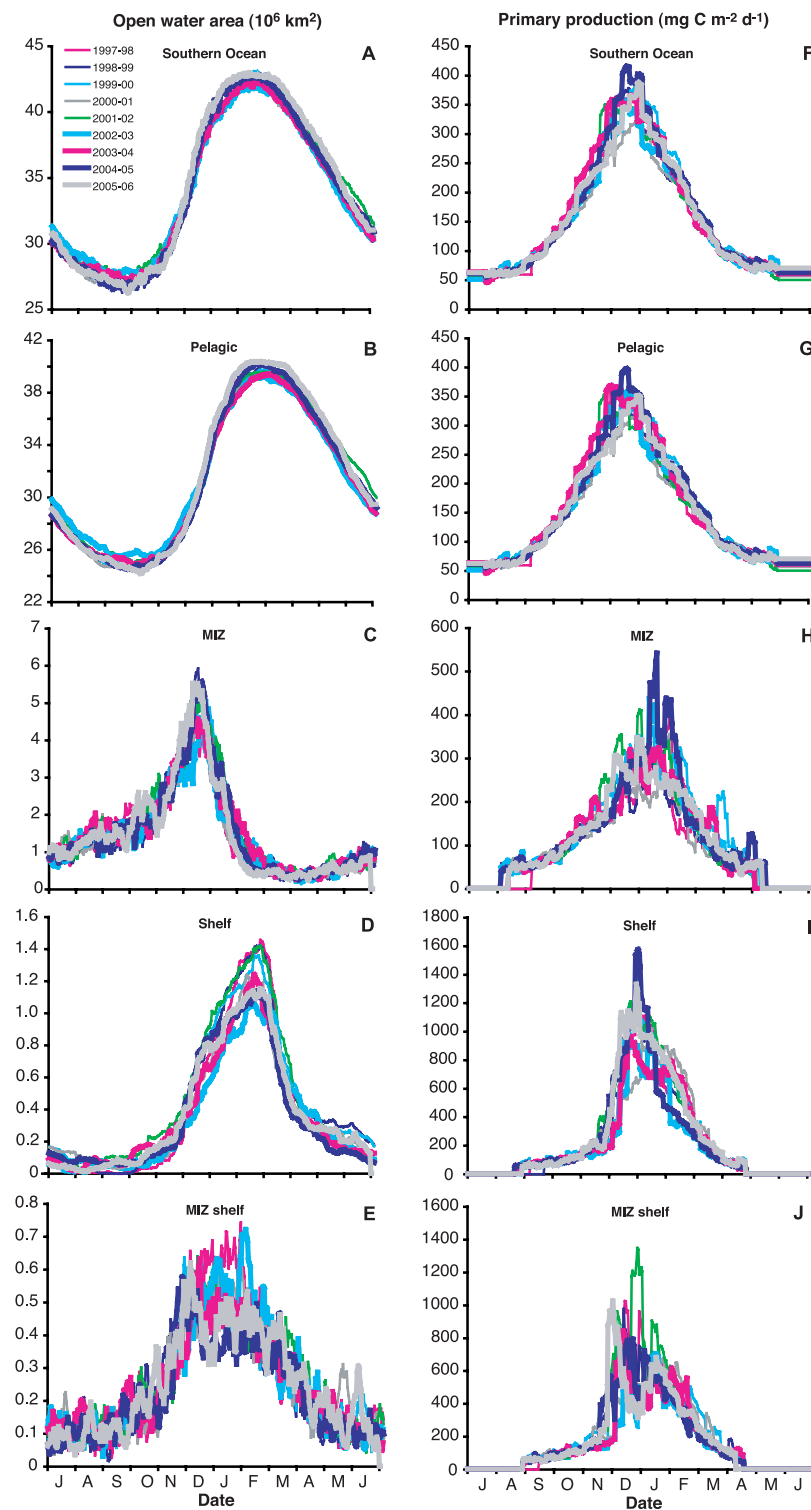


Figure 6. Annual cycles of open water area and spatially averaged daily primary production in the different ecological provinces of the Southern Ocean between 1997 and 2006.

able to the pelagic province is somewhat less than might be expected, however, given that it accounts for an average of 94% of the open water area south of 50°S (Table 2). The reason for this disparity is that the amount of production per unit area (area-normalized production) is lower in the pelagic province than in any of the other ecological prov-

vinces (Table 4). Much of the pelagic province remains ice free year-round and thus includes winter months when both the incident irradiance and rates of production are relatively low. In contrast, ecological provinces such as the shelf and MIZ-shelf are ice free only during the relatively productive spring and summer months, and consequently, have much

Table 3. Regression Coefficients for Annual Primary Production Versus Mean Open Water Area, Annual Primary Production Versus Year, and Mean Open Water Area Versus Year by Geographic Sector and Ecological Province^a

	Production Versus Open Water			Production Versus Year			Open Water Versus Year		
	R ²	p Value	Slope	R ²	p Value	Slope	R ²	p Value	Slope
<i>South Indian Ocean</i>									
Pelagic	0.002	0.915	-7.683	0.520	0.028	-0.118	0.035	0.627	-0.006
MIZ	0.179	0.257	78.75	0.056	0.539	0.142	0.061	0.520	-0.001
Shelf	0.687	0.006	191.8	0.002	0.905	0.038	0.011	0.786	0.000
MIZ-shelf	0.537	0.025	108.1	0.005	0.861	-0.012	0.169	0.272	0.000
Total	0.005	0.859	12.33	0.456	0.046	-4.236	0.038	0.615	-0.007
<i>Bellingshausen-Amundsen Sea</i>									
Pelagic	0.064	0.512	-34.44	0.221	0.201	2.493	0.000	1.000	0.000
MIZ	0.770	0.002	87.26	0.005	0.863	-0.057	0.027	0.670	-0.001
Shelf	0.542	0.024	97.22	0.050	0.564	-0.276	0.272	0.150	-0.005
MIZ-shelf	0.096	0.418	60.89	0.007	0.832	-0.042	0.396	0.070	-0.002
Total	0.314	0.117	-65.44	0.208	0.217	2.100	0.038	0.617	-0.008
<i>Ross Sea</i>									
Pelagic	0.556	0.021	112.9	0.491	0.036	7.612	0.457	0.045	0.049
MIZ	0.369	0.083	62.67	0.085	0.447	0.424	0.002	0.906	-0.001
Shelf	0.960	0.000	333.2	0.002	0.906	0.169	0.010	0.795	0.001
MIZ-shelf	0.020	0.717	78.43	0.004	0.876	-0.050	0.048	0.573	0.000
Total	0.413	0.062	116.7	0.540	0.024	8.761	0.552	0.022	0.049
<i>Southwest Pacific Ocean</i>									
Pelagic	0.006	0.848	-11.73	0.079	0.463	-1.289	0.112	0.378	0.010
MIZ	0.064	0.510	52.10	0.001	0.949	-0.026	0.017	0.736	-0.001
Shelf	0.925	0.000	208.8	0.026	0.681	-0.132	0.014	0.766	0.000
MIZ-shelf	0.756	0.002	168.9	0.014	0.762	-0.052	0.016	0.747	0.000
Total	0.003	0.893	11.52	0.058	0.532	-1.519	0.103	0.399	0.009
<i>Weddell Sea</i>									
Pelagic	0.180	0.255	69.98	0.234	0.187	7.454	0.109	0.385	-0.031
MIZ	0.454	0.047	112.0	0.396	0.069	1.235	0.070	0.492	0.003
Shelf	0.334	0.103	230.4	0.248	0.173	-1.287	0.095	0.420	-0.002
MIZ-shelf	0.543	0.024	283.4	0.271	0.151	-0.699	0.002	0.916	0.000
Total	0.192	0.239	71.19	0.149	0.306	5.968	0.099	0.409	-0.030
<i>Southern Ocean</i>									
Pelagic	0.096	0.418	-100.8	0.193	0.236	9.747	0.097	0.414	0.021
MIZ	0.635	0.010	133.6	0.124	0.353	1.607	0.001	0.945	-0.001
Shelf	0.755	0.002	267.3	0.125	0.351	-1.570	0.201	0.227	-0.006
MIZ-shelf	0.443	0.050	248.8	0.229	0.193	-0.816	0.091	0.431	-0.001
Total	0.004	0.866	19.91	0.112	0.379	8.555	0.026	0.681	0.014

^aAnnual primary production given in Tg C a⁻¹ and mean open water area given in 10⁶ km². Bolding denotes statistical significance at the 95% confidence level. In all cases, n = 9.

higher mean daily rates of production (ice-covered regions are not included in calculations of either mean or time-integrated primary production). Like the Southern Ocean as a whole, the pelagic province exhibits relatively little interannual variability in primary productivity, with annual production exhibiting a CV of only 3.5% (Table 5).

4.2.3. MIZ Province

[36] The second largest ecological province, the MIZ is also the second largest contributor to annual primary production in the Southern Ocean, averaging 86.7 ± 12.6 Tg C a⁻¹. However, because of its relatively small size throughout much of the year, the MIZ accounts for an average of 4.5% of total primary production in the Southern Ocean (Table 5). Productivity is much more temporally variable in the MIZ than in the pelagic province. Averaged over the Southern Ocean, peak production in the MIZ during the spring phytoplankton bloom ranges from 300 mg C m⁻² d⁻¹ in 2003–2004 to >550 mg C m⁻² d⁻¹ in 2004–2005 (Figure 6h). In general, daily productivity peaks about a month later (January–February) in the MIZ than in the pelagic province. As expected, peak productivity in the

MIZ lags the maximum open water area in this province by 1–2 months (Figures 6c and 6h), reflecting the time it takes for phytoplankton blooms to fully respond to the newly created ice-free waters associated with the MIZ.

Table 4. Primary Production by Geographic Sector and Ecological Province From 1997 to 2006

	Pelagic	MIZ	Shelf	MIZ	Shelf	Total
<i>Mean Daily Primary Production (mg C m⁻² d⁻¹)</i>						
Bellingshausen-Amundsen Sea	140	117	316	274		145
Ross Sea	172	192	815	485		189
South Indian Ocean	114	121	543	229		121
Southwest Pacific Ocean	130	113	343	184		132
Weddell Sea	183	202	338	294		192
Total	148	158	460	303		156
<i>Annual Primary Production (g C m⁻² a⁻¹)</i>						
Bellingshausen-Amundsen Sea	51.1	42.8	67.9	58.3		53.0
Ross Sea	62.8	70.0	179	81.9		68.9
South Indian Ocean	41.4	44.2	109	45.1		44.2
Southwest Pacific Ocean	47.3	41.1	64.1	37.3		48.2
Weddell Sea	66.6	73.7	77.0	65.2		70.2
Total	54.0	57.5	109	67.8		57.0

Table 5. Annual Primary Production by Geographic Sector and Ecological Province^a

	Pelagic	MIZ	Shelf	MIZ Shelf	Total
<i>Bellingshausen-Amundsen Sea</i>					
1997–1998	367	7.22	12.0	6.88	396
1998–1999	336	5.96	16.1	5.62	367
1999–2000	349	11.0	14.0	7.06	386
2000–2001	357	8.57	17.3	8.12	396
2001–2002	341	13.1	20.3	9.45	387
2002–2003	348	8.68	16.6	7.87	384
2003–2004	374	7.66	16.5	8.26	411
2004–2005	376	8.55	9.08	5.27	403
2005–2006	364	6.09	12.1	5.98	391
Mean	357	8.54	14.9	7.17	391
SD	14.5	2.31	3.40	1.38	12.6
<i>Ross Sea</i>					
1997–1998	410	21.1	17.0	8.78	462
1998–1999	399	27.4	28.3	8.85	492
1999–2000	398	24.3	33.5	7.34	486
2000–2001	410	19.7	19.2	5.51	465
2001–2002	417	26.4	32.5	11.3	523
2002–2003	452	20.1	2.97	3.45	483
2003–2004	483	22.7	18.1	8.74	548
2004–2005	459	32.1	28.3	8.27	548
2005–2006	426	24.6	31.2	8.28	516
Mean	428	24.3	23.4	7.84	503
SD	29.8	3.98	9.98	2.24	32.6
<i>South Indian Ocean</i>					
1997–1998	257	11.3	8.01	3.46	288
1998–1999	243	13.0	8.10	2.31	278
1999–2000	273	15.8	5.36	2.37	301
2000–2001	239	11.0	8.22	2.52	270
2001–2002	225	12.9	3.88	2.68	252
2002–2003	240	13.2	10.6	2.62	277
2003–2004	241	15.3	8.64	3.03	279
2004–2005	229	14.3	4.72	1.97	258
2005–2006	217	12.3	8.88	3.18	249
Mean	240	13.2	7.38	2.68	272
SD	16.8	1.65	2.21	0.47	17.2
<i>Southwest Pacific Ocean</i>					
1997–1998	288	7.14	3.12	2.06	304
1998–1999	292	7.53	4.35	2.69	311
1999–2000	320	14.4	8.88	4.63	352
2000–2001	285	5.99	2.77	1.93	299
2001–2002	298	13.0	8.38	5.29	327
2002–2003	309	7.14	3.73	2.70	326
2003–2004	288	9.79	3.47	2.07	307
2004–2005	289	7.68	3.92	2.59	308
2005–2006	281	8.64	3.93	2.45	299
Mean	295	9.03	4.73	2.94	315
SD	12.5	2.86	2.26	1.20	17.3
<i>Weddell Sea</i>					
1997–1998	364	31.1	30.3	14.9	464
1998–1999	421	27.2	9.05	4.44	473
1999–2000	459	31.5	12.0	4.21	519
2000–2001	357	24.8	16.1	7.38	414
2001–2002	390	39.1	15.7	3.46	457
2002–2003	395	29.3	7.57	6.41	446
2003–2004	397	33.0	6.63	2.28	451
2004–2005	448	36.2	14.6	4.75	517
2005–2006	477	41.0	11.6	5.33	546
Mean	412	32.6	13.7	5.90	477
SD	42.2	5.37	7.08	3.68	42.4
<i>Total</i>					
1997–1998	1704	71.9	71.0	35.8	1922
1998–1999	1691	81.8	70.7	25.3	1914
1999–2000	1804	98.8	77.1	26.7	2051
2000–2001	1637	68.5	63.6	25.1	1830
2001–2002	1665	107	83.1	34.6	1933

Table 5. (continued)

	Pelagic	MIZ	Shelf	MIZ Shelf	Total
2002–2003	1722	81.1	41.9	23.7	1890
2003–2004	1781	86.9	55.9	24.5	1989
2004–2005	1807	95.9	61.5	23.0	2029
2005–2006	1754	88.2	70.3	26.7	1980
Mean	1729	86.7	66.1	27.3	1949
SD	60.7	12.5	12.2	4.67	70.1

^aAnnual primary production given in Tg C a⁻¹.

[37] The Weddell Sea sector contains the largest and most productive MIZ in the Southern Ocean, averaging 32.6 ± 5.37 Tg C a⁻¹ (Table 5). This value is 25% greater than in the Ross Sea sector (24.3 ± 3.98 Tg C a⁻¹) and is at least 300% higher than in the other three geographic sectors. Interannual variability in total annual primary production within the MIZ is greatest in the Southwest Pacific Ocean sector, varying from 5.99 Tg C a⁻¹ in 2000–2001 to 14.4 Tg C a⁻¹ in 1999–2000 (Table 5).

[38] Mean area-normalized production in the MIZ is somewhat higher than in the pelagic province, averaging $158 \text{ mg C m}^{-2} \text{ d}^{-1}$, or $57.5 \text{ g C m}^{-2} \text{ a}^{-1}$ (Table 4). However, given that the MIZ has historically been considered to be a region of enhanced phytoplankton productivity, the small difference in the mean daily rate of primary production between the pelagic province and the MIZ is somewhat surprising. It should be noted that while the mean rate of production over an annual cycle in the MIZ is not much greater than in the pelagic province, the peak daily productivity values in most of the geographic sectors can be twice as high in the MIZ. For example, in the Bellingshausen-Amundsen Sea sector, mean daily production in the MIZ can exceed $1600 \text{ mg C m}^{-2} \text{ d}^{-1}$, a rate threefold higher than the corresponding peak in the pelagic province. In the other geographic sectors, a twofold greater peak production in the MIZ than in the pelagic province is not uncommon. These data suggest that while the MIZ can be a very productive marine ecosystem, this is not always the case.

4.2.4. Shelf Province

[39] Considering its small size (Figure 6d), the continental shelf (non-MIZ) is responsible for a disproportionately high fraction of primary production in the Southern Ocean, contributing 66.1 ± 12.2 Tg C a⁻¹ to the annual total (Table 5). This value is equivalent to 76% of the production of the MIZ despite the shelf being only approximately one quarter the size of the MIZ. In total, the shelf province accounts for approximately 3.5% of total phytoplankton primary production in the Southern Ocean. Mean daily primary production on the continental shelf averages $460 \text{ mg C m}^{-2} \text{ d}^{-1}$, approximately threefold greater than rates in either the MIZ or the pelagic provinces (Table 4). Similarly, mean annual production on the shelf is also relatively high ($109 \text{ g C m}^{-2} \text{ a}^{-1}$), equivalent to about twice that of the pelagic province.

[40] Productivity on the continental shelf exhibits an annual cycle unlike that of either the pelagic or the MIZ provinces. Daily rates of primary production on the shelf increase linearly and relatively slowly between August and early December throughout the Southern Ocean (Figure 6i), reaching approximately $200 \text{ g C m}^{-2} \text{ d}^{-1}$ by early December. After that time, primary productivity increases dramatically, with rates increasing fivefold to tenfold during the month of December. This rapid rise is the result of coincident increases

in phytoplankton biomass, downwelling irradiance, and surface ocean stratification during late austral spring. Of particular importance to these high rates of production are the elevated nutrients associated with the Antarctic continental shelves that allow for the accumulation of unusually high concentrations of phytoplankton biomass.

[41] Interannual variability of primary production on the shelf is higher than that of any other ecological province. With total annual production on the Southern Ocean continental shelf ranging from 41.9 Tg C a^{-1} in 2002–2003 to 83.1 Tg C a^{-1} in 2001–2002 (Table 5), the CV is 20% (the CV is only 3.5% for the pelagic province). Peak spring/summer production on the shelf averaged over the Southern Ocean varies from approximately $900 \text{ mg C m}^{-2} \text{ d}^{-1}$ in 2000–2001 to $1600 \text{ mg C m}^{-2} \text{ d}^{-1}$ in 2004–2005 (Figure 6i), with the timing of the peak varying from December to February in some sectors. Interannual variation is most extreme in the Ross Sea sector, where maximum production during the spring-summer bloom ranges from a low of $500 \text{ mg C m}^{-2} \text{ d}^{-1}$ in 2002–2003 to $>2000 \text{ mg C m}^{-2} \text{ d}^{-1}$ in 1998–1999 and 1999–2000 and total annual production varies greater than tenfold, from 2.97 Tg C a^{-1} in 2002–2003 to 33.5 Tg C a^{-1} in 1999–2000 (Table 5).

[42] Although the Ross Sea is the most interannually variable, it is also the most productive continental shelf ($23.4 \pm 9.98 \text{ Tg C a}^{-1}$), accounting for more than one third of total shelf production in the Southern Ocean (Table 5), despite comprising only 20% of ice-free shelf area (Table 2). Next in importance are the Bellingshausen-Amundsen Sea (14.9 Tg C a^{-1}) and the Weddell Sea (13.7 Tg C a^{-1}) sectors, each of which account for a little more than 20% of total shelf production in the Southern Ocean. Although the South Indian Ocean and Southwest Pacific Ocean sectors contain similar amounts of ice-free shelf area ($0.37\text{--}0.38 \times 10^6 \text{ km}^2$, Table 2), the shelf of the former sector is approximately twice as productive as that of the latter (Table 5) because of its much higher area-normalized rate of production (Table 4). Together, these two sectors account for a little less than 20% of total shelf production in the Southern Ocean.

4.2.5. MIZ-Shelf Province

[43] Due in part to its minor amount of open water area, the MIZ-shelf is the smallest contributor to annual production of the four ecological provinces, adding an average of $27.3 \pm 4.67 \text{ Tg C a}^{-1}$ (1.4%) to total phytoplankton production in the Southern Ocean. The MIZ-shelf exhibits enhanced mean daily rates of production relative to both the MIZ and pelagic provinces, averaging $303 \text{ mg C m}^{-2} \text{ d}^{-1}$, but interestingly, this value is only about 66% of the average rate on the non-MIZ continental shelf. Thus, the productivity of the MIZ-shelf is intermediate between the MIZ province and the shelf province, at least in terms of both mean daily and mean annual area-normalized production (Table 4).

[44] Lending support for the notion that the MIZ-shelf behaves more like the shelf province than like the MIZ is the fact that its annual cycle of daily production (Figure 6j) closely resembles that of the shelf province (Figure 6i), increasing slowly between August and early December, then rising rapidly before peaking in late December or January. This pattern is clearly discernable in all geographic sectors, with the possible exception of the Ross Sea, where

the typical pattern is not as obvious because of unusually early and rapid increases in productivity during some years. Peak production in the MIZ-shelf is nearly as high as in the shelf province, with mean daily production exceeding $1000 \text{ mg C m}^{-2} \text{ d}^{-1}$ throughout most of the Southern Ocean, and occasionally exceeding $1500 \text{ mg C m}^{-2} \text{ d}^{-1}$.

[45] Interannual variability is also high in this ecological province, almost as high as that of the continental shelf (Table 5). Much of this variability is associated with the rapid rise in production observed after early December. This time period is characterized by rapid changes in open water area (Figure 6e), and consequently, weekly changes in production can be large and highly variable between years (Figure 6j). Peak production during the spring/summer bloom ranges from $<800 \text{ mg C m}^{-2} \text{ d}^{-1}$ in 2004–2005 to $>1300 \text{ mg C m}^{-2} \text{ d}^{-1}$ in 2001–2002. In the Ross Sea sector, peak spring/summer production is particularly variable, ranging from $<400 \text{ mg C m}^{-2} \text{ d}^{-1}$ in 2002–2003 to $\sim 2000 \text{ mg C m}^{-2} \text{ d}^{-1}$ in 2001–2002. Like the shelf province, timing of the peak of the bloom on the MIZ-shelf also varies markedly between years, ranging from early December to mid-February in both the Weddell Sea and Ross Sea sectors.

[46] As with the shelf province, production on the MIZ-shelf is greatest in the Ross Sea sector ($7.84 \pm 2.24 \text{ Tg C a}^{-1}$), although the intersector differences in this ecological province are not nearly as large as on the shelf (Table 5). With a rate of $7.17 \pm 1.38 \text{ Tg C a}^{-1}$, the MIZ-shelf of the Bellingshausen-Amundsen Sea sector is similar to that of the Ross Sea sector, although the amount of open water area on the MIZ-shelf is much lower in the Ross Sea sector (Table 2). The Ross Sea sector compensates for its relatively smaller ice-free MIZ-shelf by having the highest area-normalized rates of production ($485 \text{ mg C m}^{-2} \text{ d}^{-1}$ and $81.9 \text{ g C m}^{-2} \text{ a}^{-1}$) of any of the geographic sectors (Table 4). Together, the Ross Sea and Bellingshausen-Amundsen Sea sectors account for 55% of the total annual production in the Southern Ocean MIZ-shelf. The Weddell Sea sector accounts for 22% of total MIZ-shelf production, while the Southwest Pacific Ocean and the South Indian Ocean sectors account for 11 and 10%, respectively.

4.3. Spatial Patterns in Primary Production

[47] To determine the physical factors most responsible for spatial and temporal patterns in annual primary production in the Southern Ocean, we calculated mean annual primary production (Figure 7a) and regressed annual production anomalies (Figure 8) against anomalies of mean annual Chl *a* concentration (Figure 9), mean annual sea ice coverage (Figure 10), and mean annual sea surface temperature (Figure 11). Not surprisingly, annual production anomalies are highly positively correlated with Chl *a* anomalies throughout the Southern Ocean (Figure 12a), with annual variations in Chl *a* explaining from $\sim 50\%$ to almost 100% of the interannual variability in mean annual production between 1997 and 2006. This high correlation is a consequence of the fact that primary productivity is calculated as the product of surface Chl *a* and the estimated phytoplankton growth rate (equation (7)). Because Chl *a* can vary by 4 orders of magnitude in the Southern Ocean, much more so than does the phytoplankton growth rate in open water when the sun is above the horizon, variations in

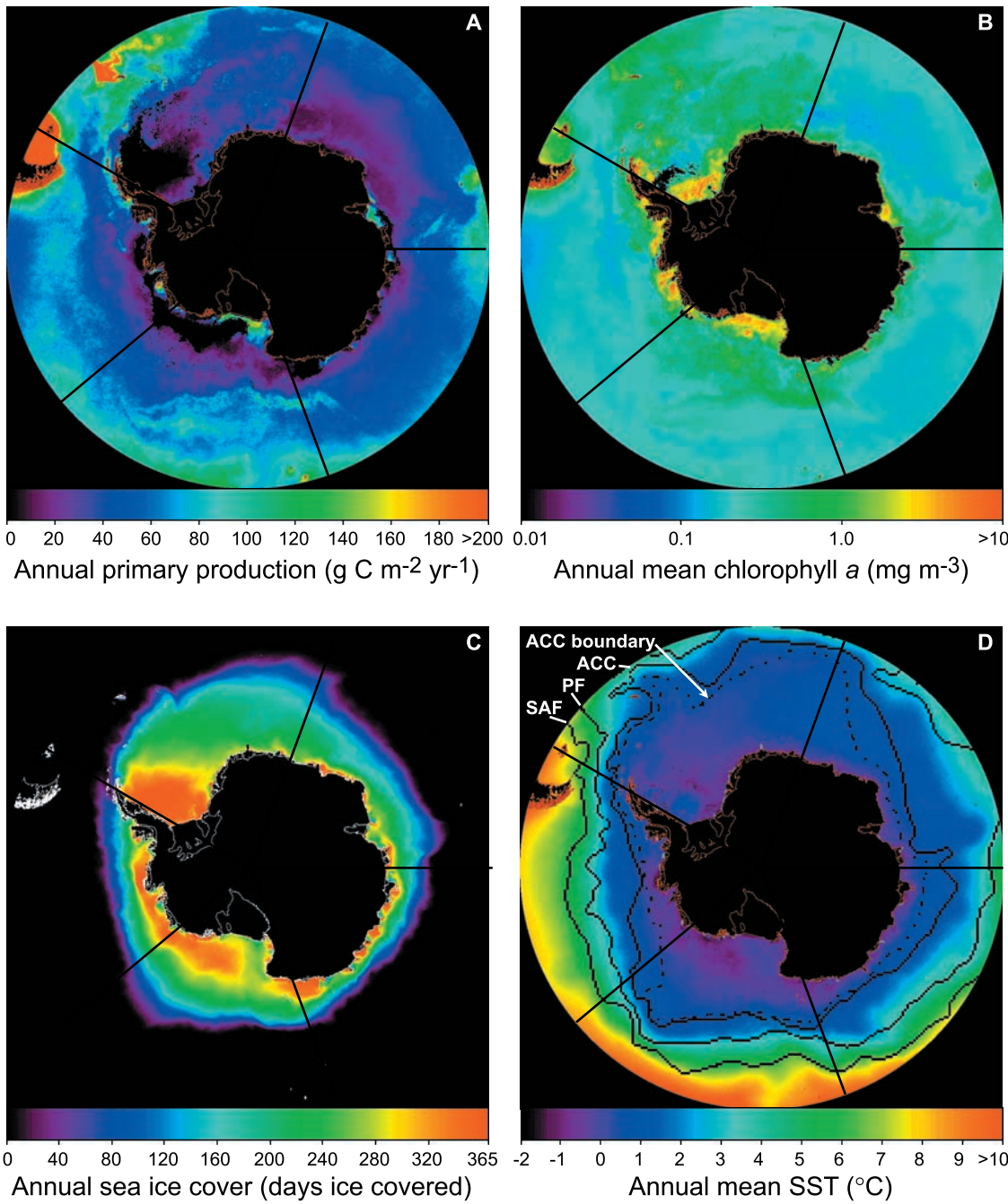


Figure 7. Annual climatologies (1997–2006) used to calculate anomalies for (a) primary production, (b) Chl *a*, (c) sea ice cover, and (d) sea surface temperature.

production are largely driven by changes in surface Chl *a*. Of course, at a given Chl *a* concentration, phytoplankton growth rate will still vary considerably depending on spatial and temporal differences in ambient irradiance and water temperature. This environmental variability explains why there is a sizable range in daily production computed by the primary production algorithm for a given Chl *a* concentration, as shown in Figure 5.

[48] Within the SIZ of the Southern Ocean, annual production anomalies (Figure 8) are also related to anomalies in sea ice distributions (Figure 10), with some locations exhibiting a positive correlation and others a negative one (Figure 12b). Negative correlations are strongest near the

coast where temperatures are lowest and sea ice persists for a longer period of time (Figures 7c and 7d). In these regions, the presence of annual sea ice typically restricts the length of the phytoplankton growth season and thus limits annual production. Consequently, the coastal zone is particularly sensitive to changes in sea ice dynamics. This pattern is clearly evident in the Southwestern Pacific Ocean sector where years with an anomalously short sea ice season, such as in 2001–2002 (Figure 10), also exhibit anomalously high annual primary production in the coastal zone (Figure 8).

[49] Farther offshore, the relationship between sea ice anomalies and annual primary production anomalies

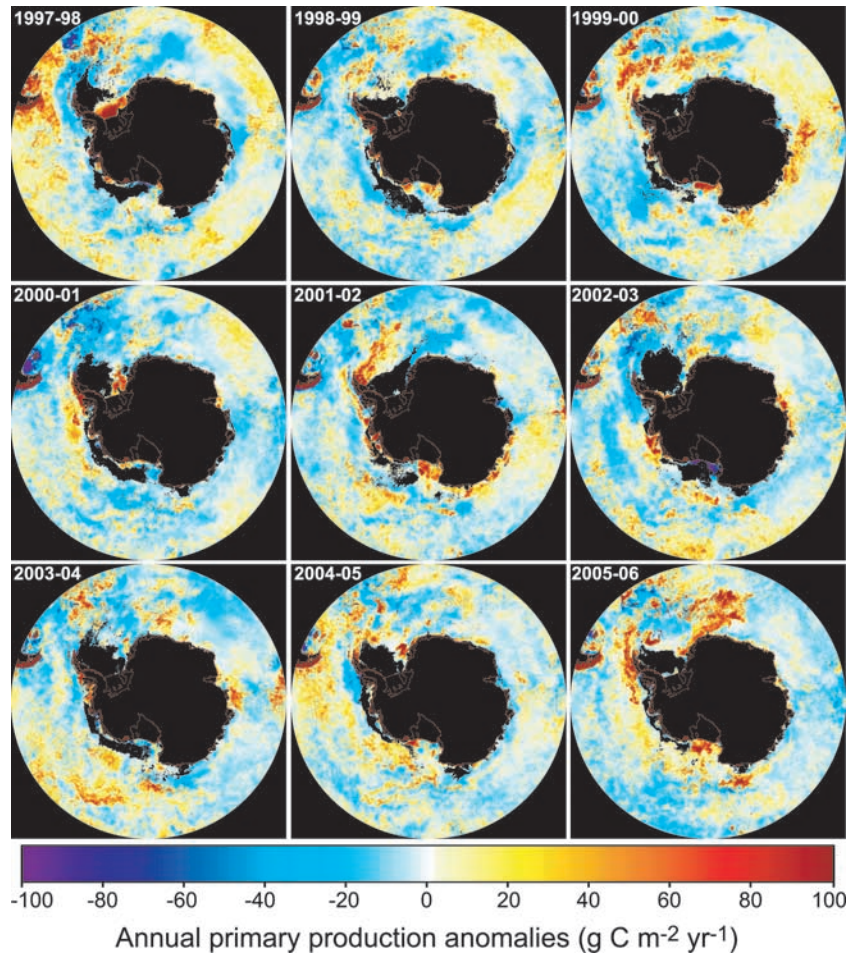


Figure 8. Anomaly maps of annual primary production for each of the 9 years of our study. Colors represent change from climatological mean shown in Figure 7a.

becomes more complex. There are obvious instances where an anomalously long sea ice season (Figure 10) leads to the expected low annual production anomaly (Figure 8), such as in both the WAP and Scotia Sea in 1997–1998. Conversely, some areas where the sea ice season is anomalously short have anomalously high annual production. Good examples include the western Weddell Sea sector in 1999–2000 and 2001–2002 and the Ross Sea sector in 2001–2002 and 2005–2006. In other regions, however, sea ice anomalies are positively correlated with annual production anomalies. This counterintuitive result stems from annual production being either higher during years when sea ice persists for a longer period of time or lower when sea ice retreats earlier in the year. This pattern is particularly evident in the western Weddell Sea sector in 1999–2000 and 2005–2006 (compare Figures 8 and 10) but is also seen in the eastern Ross Sea sector at approximately 70°S in 2001–2002. Closer inspection reveals that positive correlations between annual production anomalies and sea ice anomalies (Figure 12b) are restricted predominantly to waters where production in the MIZ province is important, such as in the Weddell Sea and offshore waters of the Ross Seas (blue areas in Figure 12d). In these waters, anomalously low sea ice will reduce both the size of the MIZ and possibly the degree of surface water stratification within any MIZ that does develop.

Because the MIZ can be more productive than the pelagic province, a loss of MIZ area will reduce annual primary production. Thus, there is generally a high correspondence between regions that exhibit a high positive correlation between annual primary production and sea ice anomalies (red areas in Figure 12b) and the approximate position of the MIZ, as can be seen clearly for the spring bloom of 1998–1999 (blue areas in Figure 12d).

[50] A map of the correlation between annual primary production anomalies (Figure 8) and annual SST anomalies (Figure 11) suggests that a complex relationship also exists between these two quantities (Figure 12c). This is likely due to the fact that SST can impact rates of production directly, through the relationship between temperature and phytoplankton metabolic rate (equation (9)), and indirectly, via its impact on surface ocean stratification and sea ice distributions. In general, waters north of the SIZ tend to exhibit a positive correlation between SST anomalies and annual production anomalies, with the highest correlation coefficients found in the Ross Sea, Bellingshausen-Amundsen Sea, and South Indian Ocean sectors (Figure 12c). SST anomalies in these regions frequently exceed $\pm 1.2^{\circ}\text{C}$, although anomalies of $\pm 0.4^{\circ}\text{C}$ are more typical. The positive correlation between anomalies of SST and annual production in these ice-free waters is the result of increased

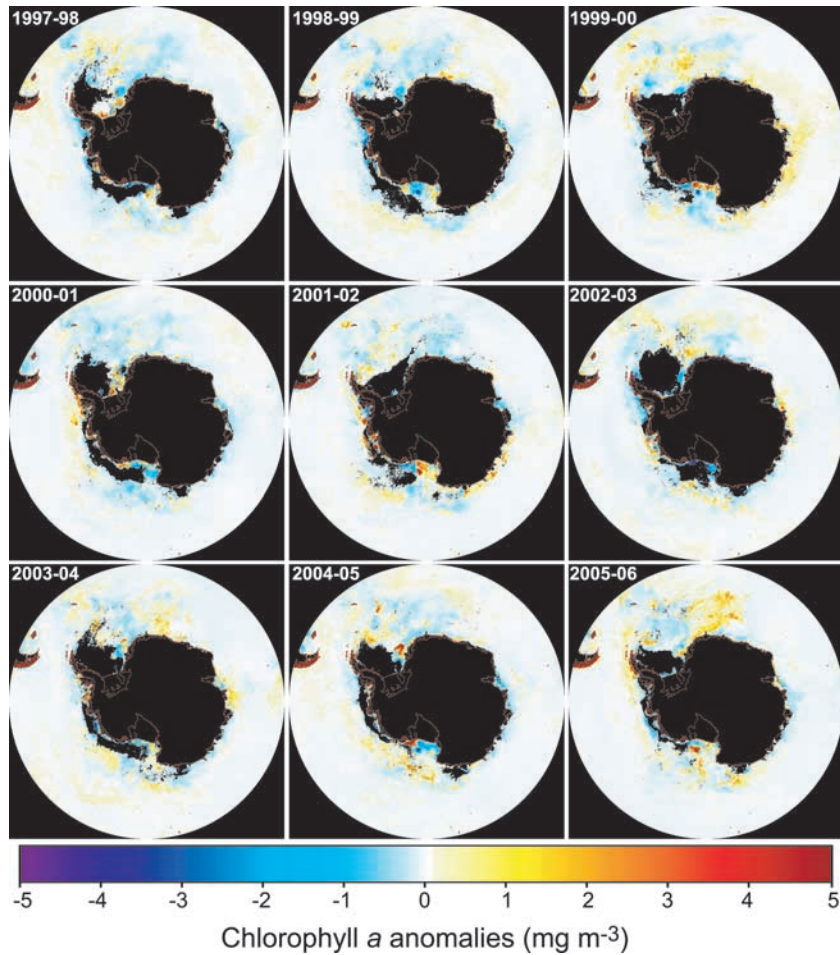


Figure 9. Anomaly maps of Chl *a* for each of the 9 years of our study. Colors represent change from climatological mean shown in Figure 7b.

phytoplankton growth rates at higher temperature. High positive correlations are also apparent within the SIZ of the Weddell Sea, the Ross Sea, and the Amundsen Sea sectors and in nearshore waters of the South Indian Ocean sector. In these regions, positive SST anomalies are frequently associated with negative sea ice anomalies (e.g., the western Weddell Sea in 1998–1999, the nearshore South Indian Ocean in 1997–1998, and the eastern Ross Sea in 2003–2004 (Figures 10 and 11)). In these cases, the high positive correlation between anomalies of SST and annual production are the result of reduced ice cover and increased light availability. Whether the ice cover is reduced because of the anomalously SST or SST is high because of reduced ice cover is not apparent.

[51] Regions exhibiting a strong negative correlation between anomalies of SST and mean annual production are predominantly restricted to the SIZ of the South Indian Ocean and a large fraction of the Southwestern Pacific Ocean sector (Figure 12c). In these waters, positive SST anomalies (Figure 11) are associated with negative mean annual production anomalies (Figure 8). There is no clear relationship between SST anomalies and sea ice anomalies in these waters, suggesting that the negative correlation between anomalies of SST and mean annual production are the result of reduced nutrient supply in waters stratified by higher temperatures, rather than by increased sea ice melt.

4.4. Temporal Trends in Annual Production

4.4.1. Secular Trends

[52] Over the 9-year time frame of this study, there is no significant temporal increase or decrease in total annual production within the Southern Ocean, with advancing year explaining only 11% of the interannual variability (Table 3). However, the passage of time has more explanatory power when the Southern Ocean is divided into geographic sectors. Both the Ross Sea and the South Indian Ocean sectors exhibit statistically significant changes in annual production between 1997 and 2006 (Table 3), with production in the Ross Sea increasing by nearly $9 \text{ Tg C a}^{-1} \text{ a}^{-1}$ ($R^2 = 0.54$, $p = 0.024$) and production in the South Indian Ocean dropping by $>4 \text{ Tg C a}^{-1} \text{ a}^{-1}$ ($R^2 = 0.46$, $p = 0.046$). The correlation between changes in annual production and year in both the Ross Sea and the South Indian Ocean sectors are most pronounced (and statistically significant) in the pelagic province (Figure 13a). The relationship between primary production and year is stronger in deep water, offshore environments than it is in the nearshore or coastal environments of the Southern Ocean (Figure 13a).

[53] In general, interannual variability in annual production is more closely tied to changes in open water area than to the passing of time. For the entire Southern Ocean, there appears at first glance to be no relationship between annual primary production and mean annual open water area ($R^2 =$

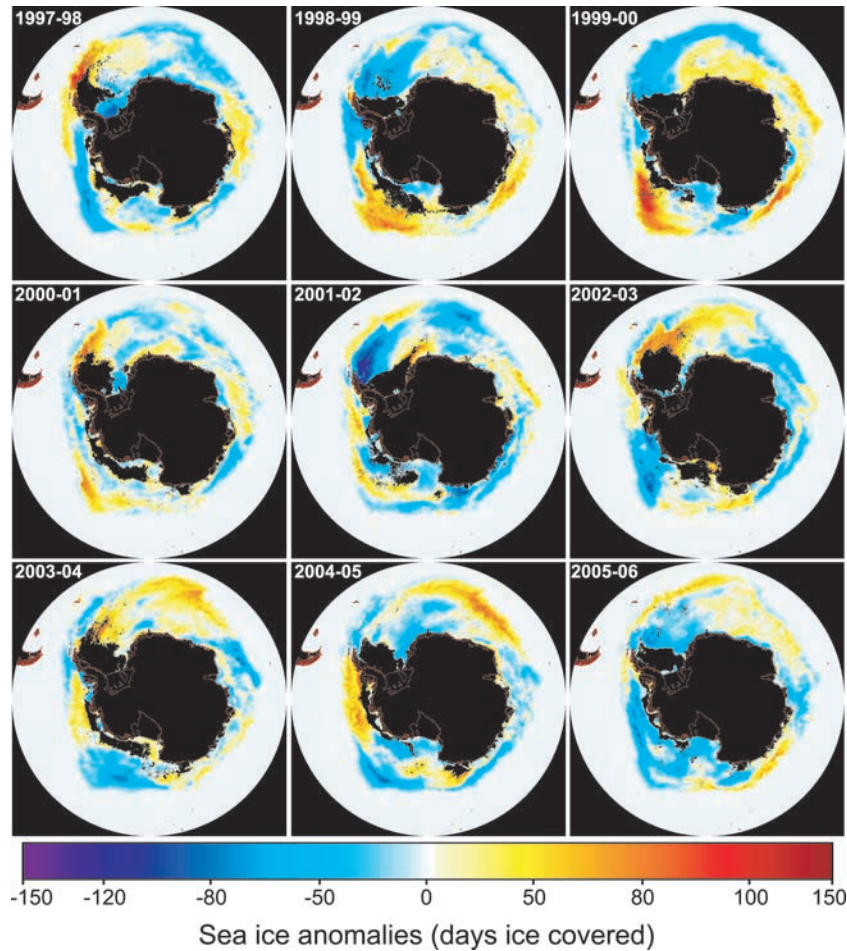


Figure 10. Anomaly maps of sea ice cover for each of the 9 years of our study. Colors represent change from climatological mean shown in Figure 7c.

0.004, Table 3). However, within the Southern Ocean there is a statistically significant relationship between annual primary production and open water area in all of the ecological provinces except for the pelagic, with the relationship between these two quantities being particularly strong in nearshore environments (Figure 13b), such as on the continental shelf ($R^2 = 0.76, p = 0.002$). Furthermore, every geographic sector contains at least one ecological province, and four out of the five contain two ecological provinces (South Indian Ocean is the lone exception), that exhibit a statistically significant relationship between annual primary production and open water area (Table 3). In all of these cases, as open water area increases, so does annual production, at a rate of approximately 100–300 Tg C for every additional million km² of open water area. For example, the shelf province exhibits a statistically significant relationship between annual production and open water area in four out of five geographic sectors, while the pelagic province varies significantly with open water area in only a single geographic sector (the Ross Sea). Thus, it appears that the poor relationship between annual primary production and advancing year is a consequence of the fact that open water area also exhibits little evidence of a secular trend through time (Figure 13c). Only the pelagic province of the Ross Sea exhibits a statistically significant change ($R^2 = 0.46, p = 0.045$) in open water area through time (Table 3).

4.4.2. Southern Annular Mode

[54] The Southern Annular Mode (SAM) is the dominant climate pattern of the Southern Ocean and is characterized by the north-south atmospheric pressure gradient and thus, the strength of the westerly winds, with the positive phase of the SAM exhibiting stronger than normal winds. Strong westerly wind anomalies associated with a positive SAM have been proposed to intensify divergence near the Antarctic Polar Front zone and result in increased upwelling of cooler, deep waters rich in nutrients, thus fueling the production of phytoplankton biomass [Lovenduski and Gruber, 2005]. This proposed pattern is consistent with our results showing that a significant relationship exists between the SAM and interannual changes in mean annual SST in the Southern Ocean ($R^2 = 0.52, p = 0.029$), with SST being lower during the high upwelling events associated with a positive SAM (Table 6). The impact of the SAM on SST seems to be particularly strong in the Ross Sea sector (slope = $-0.371, p = 0.004$) and the adjacent Southwest Pacific Ocean sector (slope = $-0.400, p = 0.015$) and much weaker in the South Indian Ocean and Weddell Sea sectors. Not surprisingly, this trend in Southern Ocean SST with SAM is most pronounced in the pelagic province ($R^2 = 0.47, p = 0.041$), which is the ecological province in closest proximity to the Antarctic divergence zone.

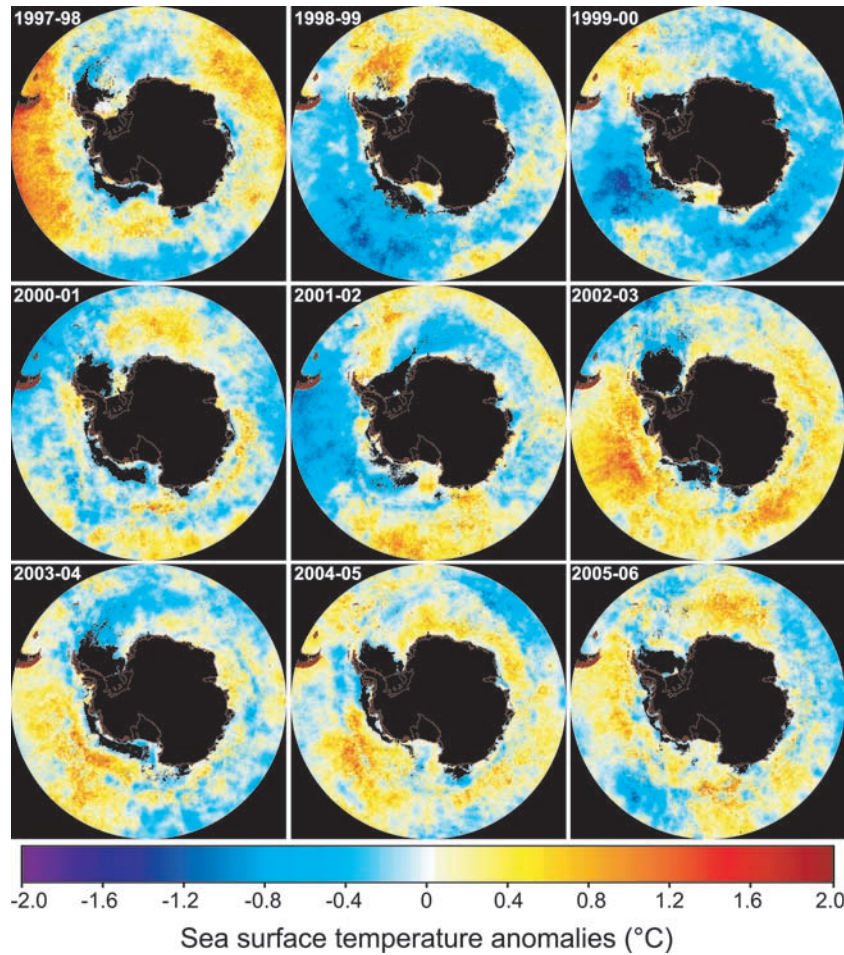


Figure 11. Anomaly maps of sea surface temperature for each of the 9 years of our study. Colors represent change from climatological mean shown in Figure 7d.

[55] Despite its correspondence with SST, the SAM explains a much smaller amount of the interannual variability in mean surface Chl *a* in the Southern Ocean (Table 6). Only the shelf province of the Ross Sea exhibited a strong and statistically significant relationship (slope = 0.826, $p = 0.009$) between interannual changes in Chl *a* and the SAM (Table 6). Similarly, there was no statistically significant relationship between total annual primary production in the Southern Ocean and the annual mean SAM index ($R^2 = 0.31$, $p = 0.123$). Although interannual trends in annual production closely track year-to-year changes in the SAM index between 1999 and 2006 (Figure 14), there were too few data points (only 9 years) for the relationship to be significant.

5. Discussion

5.1. Comparison With Previous Primary Production Estimates

[56] Annual primary production estimates reported here for all Southern Ocean waters south of 50°S are lower than previous satellite-based calculations made for this region. Using Chl *a* data from SeaWiFS and the VPGM algorithm of Behrenfeld and Falkowski [1997], Moore and Abbott [2000] estimated total production south of 50°S to be 2850 Tg C a⁻¹, 46% higher than our average for 1997–

2006 of 1949 Tg C a⁻¹. Considering that the VPGM algorithm was developed for use with global data and was not parameterized specifically for use in the Southern Ocean, this difference is not surprising. However, using monthly ocean color data from the CZCS and a productivity algorithm very similar to that used here, Arrigo *et al.* [1998a] estimated that annual production in the Southern Ocean varies from 3241 to 4414 Tg C a⁻¹, values that are 66–126% higher than our estimate. The higher estimates of production obtained by Arrigo *et al.* [1998a] are attributable to the higher Chl *a* concentrations produced by the CZCS for the Southern Ocean. Retrievals of Chl *a* by the CZCS were notoriously difficult in the Southern Ocean, a region where long atmospheric path lengths coupled with phytoplankton having unique bio-optical properties resulted in satellite-based Chl *a* estimates that were much less robust than those obtained for other ocean basins [Sullivan *et al.*, 1993]. In addition, the CZCS algorithm generated estimates of pigment concentration, rather than Chl *a*. Although attempts were made by Arrigo *et al.* [1998a] to reconcile these two variables, there has been no reliable way to convert Southern Ocean surface pigment concentration to Chl *a* over large spatial scales because of a lack of in situ pigment data. Correction factors were applied to the CZCS data to force them to conform to observations [Sullivan *et al.*, 1993], but the efficacy of these corrections was difficult

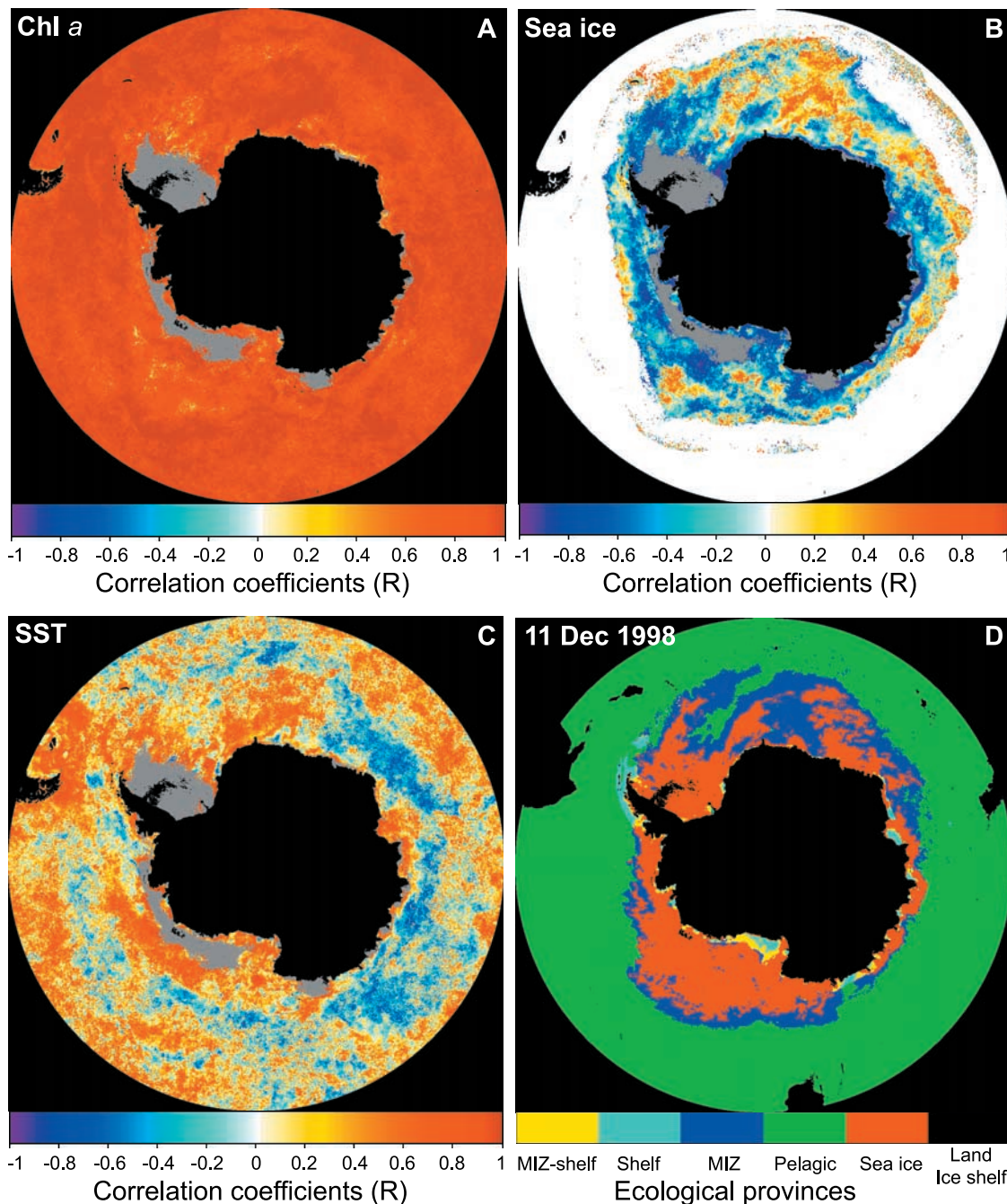


Figure 12. Maps of the correlation coefficient between mean annual primary production and (a) mean annual Chl *a*, (b) mean annual sea ice cover, and (c) mean annual sea surface temperature for the 9 years of our study. Only pixel locations, where there is data from all 9 years, are shown in color. Grey areas denote pixels where one or more years of data are unavailable. (d) Also shown is a map of the ecological provinces on 11 December 1998 to illustrate that the position of the MIZ corresponds well with areas exhibiting a high positive correlation between mean annual sea ice cover and mean annual primary production (Figure 12b).

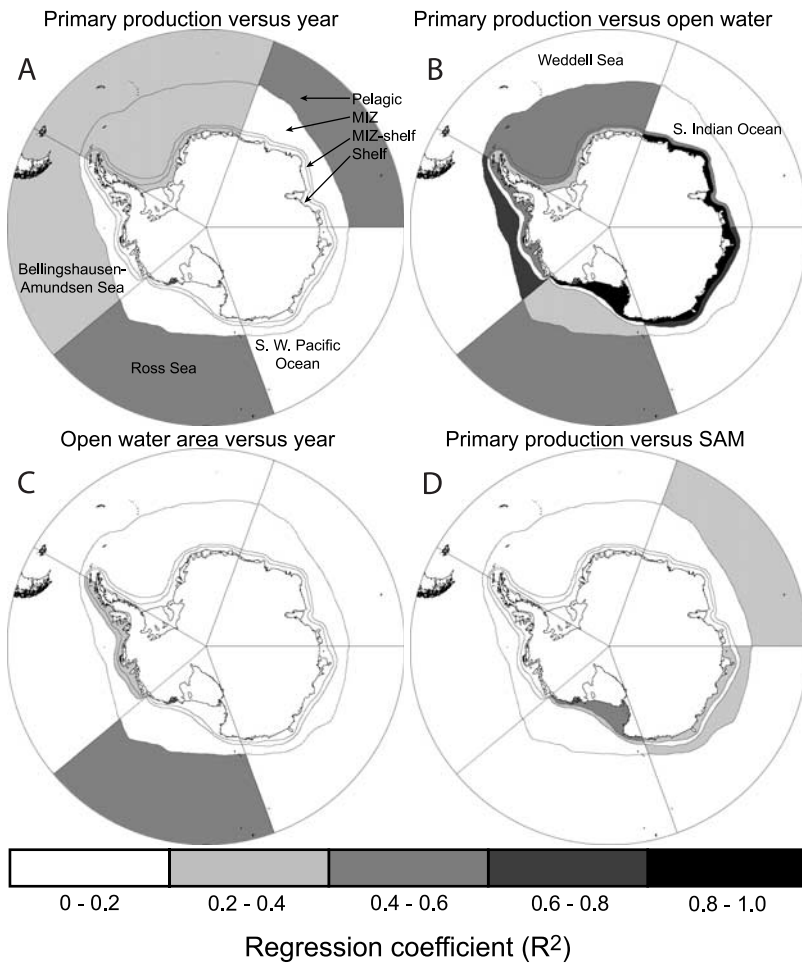


Figure 13. Schematic representation of the variation by ecological province in the strength of the correlation between (a) mean annual primary production and year, (b) mean annual primary production and mean annual open water area, (c) mean annual open water area and year, and (d) mean annual primary production and the Southern Annular Mode. The locations of the ecological provinces shown (and defined in Figure 13a) are highly idealized representations of their proximity to the coast.

to evaluate, and likely resulted in overestimates of Chl *a*, particularly in mesotrophic offshore waters [Moore and Abbott, 2000]. Therefore, although they are significantly lower, because the estimates of annual primary production presented here are based on the more reliable Chl *a* retrievals from SeaWiFS, they are likely to be more accurate than those presented by Arrigo *et al.* [1998a].

[57] Furthermore, a comparison of global output from 24 satellite-based primary production algorithms (including ours) shows that agreement between algorithms is especially poor for the Southern Ocean, with annual production ranging from 1100 to 4900 Tg C a⁻¹ and averaging 2600 Tg C a⁻¹ [Carr *et al.*, 2006]. The large divergence between algorithms was attributed primarily to the differences in the way they formulated primary production as a function of temperature. In some algorithms, production was assumed to vary independent of temperature, while in others temperature exerted a strong influence on productivity. As a result, the extremely low temperatures characteristic of many Southern Ocean waters (<0°C) resulted in estimates of primary production by the 24 algorithms that varied over a range of 372% [Carr *et al.*, 2006, Table 3].

Although the analysis by Carr *et al.* [2006] did not include an assessment of which of the 24 satellite-based estimates agreed best with in situ measurements of primary production, they noted that only two of the 24 algorithms were parameterized specifically for the Southern Ocean (ours was one) and only three of the 24 included any Southern Ocean data during model parameterization. Hence, the use of algorithms not parameterized for the Southern Ocean is likely to result in estimates of primary production that differ significantly from those presented here.

[58] Because of the increased abundance of high-quality HPLC-derived pigment data from the Southern Ocean, and the larger number of in situ estimates of daily primary production used to parameterize our algorithm, we believe that the lowered estimates of annual production in the Southern Ocean reported here are probably more realistic than past large-scale estimates. On the basis of a relatively large number of Southern Ocean analyses of SeaWiFS data [Arrigo and Van Dijken, 2004; Korb *et al.*, 2004; Garcia *et al.*, 2005; Marrari *et al.*, 2006], it is unlikely that surface Chl *a* in the Southern Ocean is being underestimated by more than 20%, and probably much less than that, partic-

Table 6. Regression Coefficients for Annual Primary Production Versus SAM, Chl *a* Versus SAM, and SST Versus SAM^a

	Production Versus SAM			Chl <i>a</i> Versus SAM			SST Versus SAM		
	R ²	p Value	Slope	R ²	p Value	Slope	R ²	p Value	Slope
<i>South Indian Ocean</i>									
Pelagic	0.233	0.187	20.12	0.350	0.092	0.022	0.016	0.749	-0.051
MIZ	0.193	0.236	1.794	0.051	0.557	0.029	0.272	0.149	-0.118
Shelf	0.162	0.282	-2.205	0.010	0.795	-0.058	0.001	0.951	0.004
MIZ-shelf	0.007	0.828	-0.098	0.103	0.398	-0.041	0.476	0.040	-0.108
Total	0.176	0.260	17.88	0.217	0.205	0.017	0.020	0.714	-0.056
<i>Bellingshausen-Amundsen Sea</i>									
Pelagic	0.083	0.450	-10.40	0.002	0.918	0.001	0.187	0.245	-0.360
MIZ	0.000	0.987	0.034	0.071	0.488	-0.101	0.208	0.217	-0.066
Shelf	0.024	0.690	-1.307	0.319	0.112	-0.240	0.008	0.824	-0.023
MIZ-shelf	0.126	0.348	-1.218	0.134	0.332	-0.144	0.028	0.665	-0.026
Total	0.065	0.277	-12.70	0.016	0.743	-0.003	0.195	0.235	-0.361
<i>Ross Sea</i>									
Pelagic	0.198	0.230	-32.83	0.022	0.700	0.004	0.495	0.021	-0.308
MIZ	0.179	0.255	4.187	0.108	0.387	-0.053	0.297	0.129	-0.096
Shelf	0.409	0.063	15.82	0.644	0.009	0.826	0.256	0.164	-0.308
MIZ-shelf	0.320	0.111	3.144	0.236	0.185	0.387	0.209	0.215	0.059
Total	0.002	0.909	3.607	0.310	0.119	0.035	0.726	0.004	-0.371
<i>Southwest Pacific Ocean</i>									
Pelagic	0.087	0.439	9.185	0.421	0.058	0.020	0.594	0.015	-0.393
MIZ	0.295	0.130	3.855	0.202	0.225	0.133	0.278	0.144	-0.094
Shelf	0.284	0.139	2.995	0.268	0.153	0.202	0.020	0.714	-0.026
MIZ-shelf	0.165	0.276	1.206	0.232	0.189	0.130	0.144	0.313	-0.049
Total	0.167	0.274	17.50	0.385	0.074	0.025	0.564	0.012	-0.400
<i>Weddell Sea</i>									
Pelagic	0.183	0.250	44.80	0.005	0.854	0.006	0.032	0.111	0.057
MIZ	0.008	0.812	1.235	0.320	0.112	0.069	0.562	0.020	0.110
Shelf	0.002	0.915	0.701	0.016	0.741	0.091	0.549	0.022	0.182
MIZ-shelf	0.016	0.745	-1.154	0.032	0.642	0.118	0.023	0.697	0.214
Total	0.220	0.201	49.40	0.017	0.733	0.011	0.429	0.055	0.067
<i>Southern Ocean</i>									
Pelagic	0.102	0.401	48.14	0.308	0.120	0.014	0.472	0.041	-0.247
MIZ	0.139	0.322	11.58	0.039	0.607	0.013	0.244	0.177	-0.060
Shelf	0.408	0.064	19.29	0.343	0.096	0.155	0.103	0.399	0.023
MIZ-shelf	0.057	0.532	2.788	0.224	0.197	0.130	0.010	0.798	0.005
Total	0.305	0.123	95.98	0.428	0.055	0.020	0.516	0.029	-0.252

^aAnnual primary production given in Tg C a⁻¹. Bolding denotes statistical significance at the 95% confidence level.

ularly in the open ocean where pigment concentrations are relatively low and account for the bulk of production. Furthermore, rates of primary production for a given concentration of Chl *a* calculated by our algorithm agree very well with a wide range of observations made in the Southern Ocean (Figure 5). If true, the Southern Ocean is considerably less productive than has been assumed over much of the past decade, with annual production rates equivalent to approximately 41–70% of previous estimates [Longhurst *et al.*, 1995; Arrigo *et al.*, 1998a; Moore and Abbott, 2000; Reuer *et al.*, 2007]. Rather than representing approximately 10% of global marine primary production [Arrigo *et al.*, 1998a], our results suggest that the Southern Ocean accounts for less than 5% of this amount.

5.2. MIZ's Productivity

[59] Given that the MIZ historically has been considered to be a region of enhanced primary productivity, the small differences in both daily and annual area-normalized rates of production between the generally low productivity pelagic province and the MIZ province are somewhat surpris-

ing. Although some of this similarity may be attributable to the operational definition of a MIZ used in the present study, this is not likely to be the primary reason. We defined the MIZ province as consisting of those pixels that have been ice-free for no longer than 14 consecutive days. Once this threshold has been reached, the pixel is redefined as either a pelagic or MIZ-shelf pixel, depending upon water depth. If our 14-day threshold is much shorter than the lifetime of a typical MIZ, any productivity that should be attributed to the MIZ will have been associated with the pelagic or MIZ-shelf province. The seriousness of this underestimate of MIZ production will depend on how long it takes for phytoplankton to bloom after the sea ice retreats. If the MIZ phytoplankton bloom takes longer than 14 days to reach its peak, production in the MIZ will be underestimated using a 14-day threshold. Lancelot *et al.* [1991] noted that in the Weddell-Scotia Sea, the region of maximum water column Chl *a* in the MIZ was consistently located within 0.5° (56 km) of the ice edge during the spring of 1988. Given a rate of sea ice retreat of 6–14 km d⁻¹ (see section 2.2), peak Chl *a* concentrations must have been reached

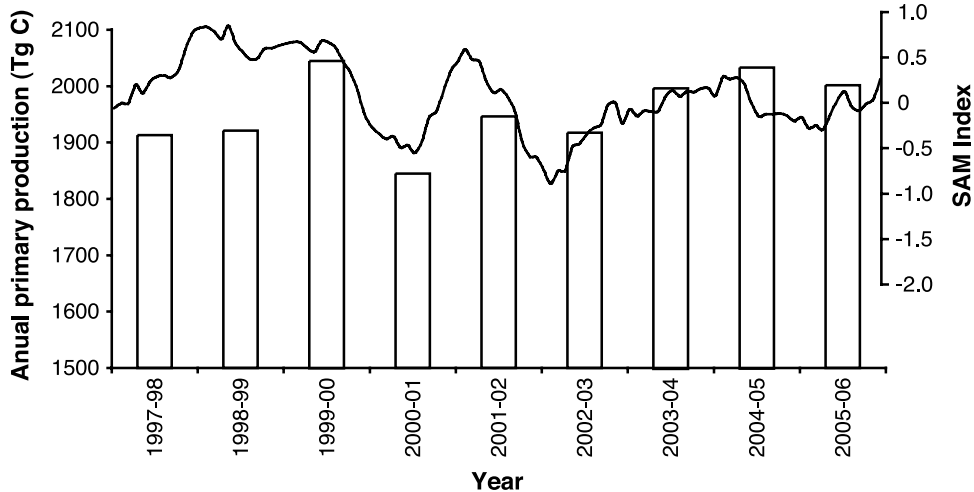


Figure 14. Total annual primary production in the Southern Ocean between 1997 and 2006 plotted along with variability in the Southern Annular Mode Index. Monthly SAM data were obtained from the NOAA Climate Prediction Center (http://www.cpc.noaa.gov/products/precip/CWlink/daily_ao_index/ao/aao_index.html) and smoothed using a 3-month moving average. Although the relationship between SAM and annual primary production is not significant ($R^2 = 0.31, p = 0.12$), changes in both variables are quite similar.

4–9 days after sea ice retreat, well within our 14-day threshold. This conclusion is supported by the large number of high productivity events associated with the MIZ during spring and summer in our study (Figure 6h), suggesting that phytoplankton are attaining high levels of biomass and rates of production within the 14-day threshold used to define the MIZ.

[60] In two previous studies of primary production in the Southern Ocean, the MIZ was defined as the region of open water in a given month that had been ice covered the previous month [Arrigo *et al.*, 1998a; Moore and Abbott, 2000]. Both of these studies calculated productivity (and the size of the MIZ) from monthly mean data, including both sea ice and Chl *a* data, and thus the MIZ was assumed to persist for approximately 30 days, twice as long as was assumed in the present study. In the investigation by Arrigo *et al.* [1998a], the MIZ accounted for 9.5% of total primary production in the Southern Ocean, much higher than the 4.4% estimated for the MIZ in the present study. It is unlikely however, that this difference can be attributed to the longer-lived MIZ assumed by Arrigo *et al.* [1998a]. This is because Moore and Abbott [2000] also used a 30-day threshold for the MIZ and they estimated a mean rate of production within the MIZ of $54.2 \text{ g C m}^{-2} \text{ a}^{-1}$, very close to our estimate of $57.5 \text{ g C m}^{-2} \text{ a}^{-1}$. Moreover, the MIZ in their study accounted for 3.3% of total annual primary production, much less than the estimate of 9.5% by Arrigo *et al.* [1998a] who used the same 30-day threshold, and even slightly lower than the estimate of 4.4% made here using a 14-day threshold.

[61] These results indicate that the calculated production of the MIZ is more closely tied to the Chl *a* field used as algorithm input than it is to the assumed lifetime of the MIZ. The present study and the study by Moore and Abbott [2000] both used SeaWiFS data to specify phytoplankton distributions and obtained similar results for MIZ production (despite using MIZ lifetimes of 14 and 30 days, respectively) while Arrigo *et al.* [1998a] used CZCS data

and obtained much higher estimates of MIZ production (despite using the same MIZ lifetime as that used in the present study). Chl *a* in regions of high sea ice cover was often overestimated by the CZCS because of incomplete masking of sea ice contaminated pixels [Arrigo and McClain, 1995]. This problem would have been most serious in the MIZ where sea ice can be present at concentrations low enough to be missed by the sea ice masking algorithm. Largely corrected in the SeaWiFS data, overly high estimates of Chl *a* by the CZCS in the MIZ may explain why estimates of MIZ production by Arrigo *et al.* [1998a] are so much higher than those presented here and by Moore and Abbott [2000].

[62] Why then is the MIZ only slightly more productive than the pelagic province? If not an artifact of our analyses, then the lower than expected productivity of much of the MIZ must be attributable to conditions not always being conducive for intense phytoplankton blooms. While it is true that maximum rates of daily primary production are much higher in the MIZ (Figure 6h) than in the pelagic province (Figure 6g), it is also true that the minimum values in the MIZ are substantially lower than in the pelagic. This trend applies to all geographic sectors as well as during the peak spring-summer phytoplankton bloom season. For example, while maximum rates of primary production in the MIZ of the Bellingshausen-Amundsen Sea often exceed $600 \text{ mg C m}^{-2} \text{ d}^{-1}$ for short periods of time, more often, rates of production during the peak of the spring bloom (December–January) are in the range of $200\text{--}250 \text{ mg C m}^{-2} \text{ d}^{-1}$. In contrast, although there were not as many high productivity bloom events in the pelagic province of the Bellingshausen-Amundsen Sea, primary production in late December–early January exceeded $300 \text{ mg C m}^{-2} \text{ d}^{-1}$ during each of the 9 years of our study. Thus, although the MIZ province experiences more high productivity blooms than the pelagic, it is also characterized by lower nonbloom rates of production.

[63] One explanation for this is that much of the MIZ of the Southern Ocean either never develops a well-stratified upper mixed layer or the mixed layer is destroyed by wind-driven turbulent mixing before a phytoplankton bloom can form [Fitch and Moore, 2007]. By definition, the MIZ is an area of open water within the SIZ that has recently been covered with sea ice. While still ice covered, there is little chance of appreciable phytoplankton growth because of low light transmission through the snow, sea ice, and associated particulate material [Arrigo et al., 1991], and phytoplankton abundance will be low. Once the sea ice has left an area because of advection and/or melting, phytoplankton can grow, given sufficient light and nutrients, although initial Chl *a* concentrations will be low unless there is an appreciable contribution of algal cells from melting sea ice. In the absence of a well-stratified mixed layer, phytoplankton biomass and rates of primary production in the MIZ will remain low. Similarly, even when a stratified mixed layer does develop, if it does so in offshore waters that are low in micronutrients such as Fe (macronutrients are in ample supply over most of our study region), nutrients will be rapidly exhausted and primary production also will be low. As can be seen from the small fraction of total SIZ area exhibiting a strong positive correlation between primary production and sea ice distributions (Figure 12b, sea ice and primary production are only positively correlated in the MIZ), conditions favoring phytoplankton blooms in the MIZ are relatively uncommon and account for a small fraction of total MIZ area. Thus, while the MIZ is large and has the potential to be biologically productive, physical conditions there are seldom conducive to the development of intense, longer-lived phytoplankton blooms.

[64] In addition to daily rates of primary production in much of the MIZ that are relatively low because of unfavorable growth conditions, annual rates are also low. This is due in part to the modest daily rates, which are, on average, only 7% higher than in the pelagic province, but also to the shorter growing season characteristic of the MIZ. The impact of growing season can be seen most clearly by comparing distributions of Chl *a* (Figure 7b) and annual primary production (Figure 7a). Despite the fact that the SIZ and MIZ have mean Chl *a* concentrations that are higher than in pelagic waters north of the SIZ, annual production in the MIZ and the pelagic province are similar in magnitude (57.5 and 54.0 g C m⁻² a⁻¹, respectively). The high Chl *a* concentrations in the SIZ are somewhat misleading because they only reflect values when waters have become ice free; they do not include concentrations below the sea ice that would undoubtedly reduce the annual mean substantially. Nevertheless, the length of the growing season, which can be inferred from Figure 7c by subtracting a given pixel value from the number 365 (or 366 for leap years), is substantially shorter in the SIZ and MIZ than it is throughout much of the pelagic zone; most of the SIZ and MIZ have growing seasons that are less than half as long as those north of the SIZ. Consequently, rates of annual production in the MIZ differ little from corresponding values in the pelagic province. Similarly, a reduced growing season in the MIZ also explains much of why productivity in the MIZ-shelf province is so much lower than in the (non-MIZ) shelf (Tables 4 and 5).

5.3. Interannual Variability in Primary Productivity

[65] Annual primary production in the Southern Ocean exhibited a surprisingly small amount of interannual variability between 1997 and 2006, varying by only $\pm 11\%$ (computed as [maximum – minimum]/mean). This is significantly less interannual variability than has been measured in other ocean basins. For example, annual net primary production varied by 30% or more over large stretches of the tropical Pacific Ocean between 1999 and 2004 [Behrenfeld et al., 2006]. Much of this variability is attributable to ENSO-driven changes in upper ocean temperature and stratification, changes that are not manifested nearly so severely in the Southern Ocean. Lomas and Bates [2004] documented an extremely high degree of interannual variability in primary production (121%) in the western north Atlantic tropical gyre from 1992 to 2000. This large variability derives primarily from interannual changes in nutrient input via deep convective mixing driven by the passage of storms [Steinberg et al., 2001]. Because nutrient inventories in the relatively shallow upper mixed layer of the tropical gyres are so low, phytoplankton growth rates in these waters are particularly sensitive to changes in nutrient input. This sensitivity to nutrient supply is in stark contrast to the Southern Ocean where mixed layers are deep, relative changes in nutrient inventories of the upper ocean are modest, and variability in production is attributable primarily to changes in light environment (via variations in sea ice extent). A good example of this is the WAP where the observed order of magnitude changes in primary production from year-to-year are related to the amount of open water within the annual ice pack [Ducklow et al., 2006].

[66] Interannual variability in annual production in the Southern Ocean also is lower than in other polar and subpolar waters. For instance, interannual variability of primary production in the North Sea is around 15% [Skogen and Moll, 2000], slightly higher than the 11% reported here. More significantly, estimates of annual primary production in the Arctic Ocean (all waters north of the Arctic Circle) made over the same 9-year period as the present study varied from 375 to 483 Tg C a⁻¹, an interannual range of 26% [Pabi et al., 2008]. These interannual differences in Arctic primary production are attributable primarily to the dramatic changes in ice-free area over the past decade, which has increased by $\sim 75,000 \text{ km}^2 \text{ a}^{-1}$ since 1998. As was observed in the present study of the Southern Ocean, interannual changes in Arctic waters are most dramatic on the continental shelves, which make up a much larger fraction of total area in the Arctic (53%) than they do in the Antarctic.

[67] Although interannual changes in the amount of open water in the Southern Ocean were not significantly correlated with annual rates of primary production (Table 3), a strong relationship exists between the degree of interannual variability in open water area in a given region and interannual variability in annual primary production (interannual variability is quantified as the ratio of the maximum to the minimum mean annual value for each geographic sector and ecological province, Figure 15). Not surprisingly, regions exhibiting the greatest interannual range in open water area (e.g., the Ross Sea shelf) also exhibited the largest range in annual primary production. What is surprising is that the data from all of the geographic sectors and

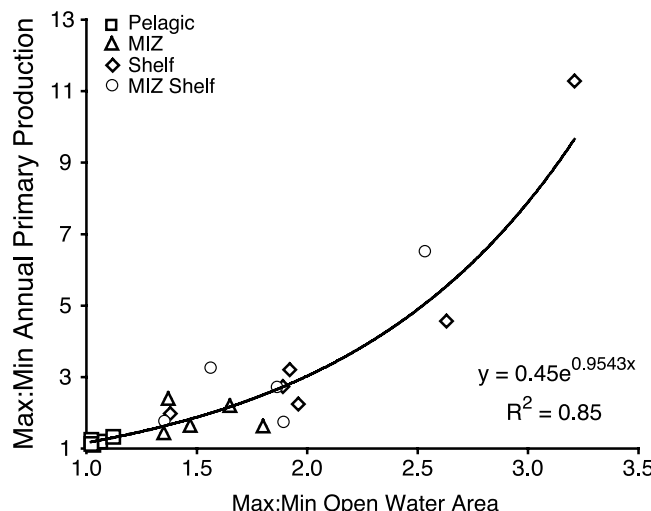


Figure 15. Ratio of the maximum to the minimum open water area during 1997–2006 regressed against the ratio of the maximum to minimum annual production for each geographic sector and ecological province.

ecological provinces can be explained by a single relationship $Y = 0.45 \exp(0.9543X)$, $R^2 = 0.85$, $p < 0.001$, despite the fact that each region exhibits a very different relationship between annual primary production and mean annual open water area (Table 3). Two important conclusions can be drawn from this relationship. First, interannual variations in production are driven primarily by changes in sea ice cover, although changes in nutrient delivery (most likely iron) to surface waters induced by processes associated with atmospheric variability (e.g., SAM) also likely play a role. Second, the relationship between min:max open water area and min:max annual production (integrated over the Southern Ocean) is not linear, with annual primary production changing more rapidly than the change in open water area. This reflects the fact that when open water increases, both the total area suitable for phytoplankton growth and the area-normalized rates of production increase.

[68] Open water in the Arctic has increased dramatically since 2002, with an associated increase in annual primary production [Pabi et al., 2008]. Similar secular trends have not been observed in the Antarctic, with the exception of the Bellingshausen-Amundsen Sea, where increasing temperatures between 1957 and 1998 are associated with a substantial loss of sea ice [Turner et al., 2007]. Increases in temperature in the Antarctic Peninsula region and a slight cooling within much of the Antarctic interior have been attributed to a shift toward a positive phase of the SAM that began in 1957, the result of decreased stratospheric ozone concentrations. This loss of ozone has generated colder tropospheric temperatures over the Antarctic continent, a larger meridional pressure gradient, and increased westerly winds near 60°S [Thompson and Solomon, 2002]. These more intense westerlies are thought to warm the Antarctic Peninsula by decreasing the incidence of cold air outbreaks from the Antarctic interior, leading to increased advection of warmer air from the Southern Ocean [Thompson and Solomon, 2002]. However, this proposed scenario is complicated by the fact that the climate of the Antarctic

Peninsula also is strongly affected by teleconnections with the tropics [Turner et al., 2007]. During El Niño, higher mean sea level pressure over the Bellingshausen Sea results in a cooling of the Antarctic Peninsula. Furthermore, recent El Niño events have been more intense and more frequent, which would be expected to result in cooling trend in the region, rather than the rapid warming that has been measured over the past few decades [Turner et al., 2007]. It is clear that the causes of the warming in the Antarctic Peninsula region have not yet been fully elucidated.

[69] The lack of a secular trend in both sea ice extent and phytoplankton productivity likely can be attributed to the lack of a warming trend over much of the Antarctic because of the shift to a positive phase of the SAM over the last half century. This shift has resulted in little or no change in temperature over much of the Antarctic, with the exception of the Antarctic Peninsula, and no long-term trend in sea ice concentration. Because the recent long-term shift to a positive SAM has been tied to reductions in stratospheric ozone resulting from increased CFC production, it is possible that warming and loss of sea ice in the Southern Ocean would have been more extreme in recent decades had the Antarctic ozone hole not developed [Thompson and Solomon, 2002].

5.4. Future Changes in Southern Ocean Primary Production

[70] Changes in Southern Ocean circulation and biogeochemistry have proven to be difficult to predict because of a limited observational database and an inability of many large-scale models to accurately represent important physical, chemical, and biological processes. In a comparison of 18 coupled climate models included in the IPCC Fourth Assessment Report, Russell et al. [2006a] noted the wide range in model predictions of water mass transformations and the strength and position of the westerly wind belt, key components in the ability to predict anthropogenic CO₂ uptake and changes in biological productivity. One area of general agreement among models is that stratification of the surface Southern Ocean is likely to increase over the next century in response to changes in atmospheric CO₂ and temperature [Sarmiento et al., 1998; Caldeira and Duffy, 2000; Le Quéré et al., 2007]. This increase in stratification will reduce both the ability of the surface ocean to remove atmospheric CO₂ and the flux of nutrients from the deep ocean, thereby reducing phytoplankton growth and productivity. In a recent model that was better able to simulate the poleward intensification of the westerly winds [Russell et al., 2006b], it was predicted that storage of heat and anthropogenic CO₂ would actually increase in the future because of a larger outcrop area of the dense waters around Antarctica and more intense divergence, thereby counteracting the effect of increased stratification of most of the Southern Ocean.

[71] This predicted increase in divergence could increase the flux of micronutrients into the Polar Front zone and into waters further south, thereby increasing phytoplankton growth and productivity. Although the magnitudes of Chl *a* concentrations and primary production have been shown here to respond weakly, but positively, to increased divergence associated with the SAM (Table 6), these effects might be much larger under conditions of increased divergence in the future. On the other hand, the meridional pressure gradient that has intensified in recent decades because of the strato-

spheric cooling associated with the Antarctic ozone hole [Thompson and Solomon, 2002] may diminish in coming years as stratospheric CFC concentrations drop and the Antarctic ozone hole dissipates. How the balance between these two large global perturbations will impact biogeochemistry in the Southern Ocean has yet to be determined.

[72] Finally, in addition to aforementioned changes in the Southern Ocean predicted for the upcoming century (increased westerly winds, stronger Antarctic divergence, increased surface ocean stratification) is a 17–31% reduction in sea ice extent, assuming a doubling of atmospheric CO₂ by 2100 [Rind et al., 1997; Meehl et al., 2000]. Arrigo and Thomas [2004] predicted that a 25% decrease in sea ice would result in a 10% increase in total primary production, with increases in production north of the ice edge outpacing losses in the diminished areas of the MIZ and SIZ. However, their analysis assumed that rates of production in the MIZ were substantially higher than those in the pelagic province. Our results (and similar results found by Moore and Abbott [2000]), suggest that this is not the case, that average rates of daily primary production in the MIZ are very similar to those in the pelagic province. Thus, the predicted losses of production due to a diminished size of the MIZ will not be as large as those assumed by Arrigo and Thomas [2004]. Consequently, the net increase in total production in the Southern Ocean in response to a reduced sea ice cover should be a few percent larger than the 10% predicted by Arrigo and Thomas [2004].

[73] **Acknowledgments.** This research was supported by DOE grants DE-FG02-04ER63896 and DE-FG02-04ER63891 and NASA grant NNG05GC92G to K. Arrigo.

References

- Arrigo, K. R., and C. R. McClain (1995), Cloud and ice detection at high latitudes for processing of CZCS imagery, *NASA Tech. Memo., TM-104566*, vol. 28, 8–12.
- Arrigo, K. R., and C. W. Sullivan (1994), A high resolution bio-optical model of microalgal growth: Tests using sea ice algal community time series data, *Limnol. Oceanogr.*, **39**, 609–631.
- Arrigo, K. R., and D. Thomas (2004), Large scale importance of sea ice biology in the Southern Ocean, *Antarct. Sci.*, **16**(4), 471–486, doi:10.1017/S0954102004002263.
- Arrigo, K. R., and G. L. Van Dijken (2003), Phytoplankton dynamics within 37 Antarctic coastal polynyas, *J. Geophys. Res.*, **108**(C8), 3271, doi:10.1029/2002JC001739.
- Arrigo, K. R., and G. L. Van Dijken (2004), Annual changes in sea ice, chlorophyll *a*, and primary production in the Ross Sea, Antarctica, *Deep Sea Res. Part II*, **51**, 117–138, doi:10.1016/j.dsro.2003.04.003.
- Arrigo, K. R., and G. L. Van Dijken (2007), Interannual variation in air-sea CO₂ flux in the Ross Sea, Antarctica: A model analysis, *J. Geophys. Res.*, **112**, C03020, doi:10.1029/2006JC003492.
- Arrigo, K. R., C. W. Sullivan, and J. N. Kremer (1991), A bio-optical model of Antarctic sea ice, *J. Geophys. Res.*, **96**, 10,581–10,592, doi:10.1029/91JC00455.
- Arrigo, K. R., D. L. Worthen, A. Schnell, and M. P. Lizotte (1998a), Primary production in Southern Ocean waters, *J. Geophys. Res.*, **103**, 15,587–15,600, doi:10.1029/98JC00930.
- Arrigo, K. R., D. H. Robinson, M. P. Lizotte, D. L. Worthen, and B. Schieber (1998b), Bio-optical properties of the southwestern Ross Sea, *J. Geophys. Res.*, **103**, 21,683–21,695, doi:10.1029/98JC02157.
- Arrigo, K. R., G. R. DiTullio, R. B. Dunbar, M. P. Lizotte, D. H. Robinson, M. VanWoert, and D. L. Worthen (2000), Phytoplankton taxonomic variability and nutrient utilization and primary production in the Ross Sea, *J. Geophys. Res.*, **105**, 8827–8846, doi:10.1029/1998JC000289.
- Barbini, R., F. Colao, R. Fantoni, L. Fiorani, N. V. Kolodnikova, and A. Palucci (2006), A Laser remote sensing calibration of ocean color satellite data, *Ann. Geophys.*, **49**(1), 35–43.
- Behrenfeld, M. J., and P. G. Falkowski (1997), Photosynthetic rates derived from satellite-based chlorophyll concentration, *Limnol. Oceanogr.*, **42**(1), 1–20.
- Behrenfeld, M. J., R. T. O’Malley, D. A. Siegel, C. R. McClain, J. L. Sarmiento, G. C. Feldman, A. J. Milligan, P. G. Falkowski, R. M. Letelier, and E. S. Boss (2006), Climate-driven trends in contemporary ocean productivity, *Nature*, **444**(7120), 752–755, doi:10.1038/nature05317.
- Boyd, P. W., et al. (2000), A mesoscale phytoplankton bloom in the polar Southern Ocean stimulated by iron fertilization, *Nature*, **407**, 695–702, doi:10.1038/35037500.
- Broecker, W. S. (1991), The great ocean conveyor, *Oceanography*, **4**, 79–89.
- Caldeira, K., and P. B. Duffy (2000), The role of the Southern Ocean in uptake and storage of anthropogenic carbon dioxide, *Science*, **287**, 620–622, doi:10.1126/science.287.5453.620.
- Carr, M.-E., et al. (2006), A comparison of global estimates of marine primary production from ocean color, *Deep Sea Res. Part II*, **53**(5–7), 741–770, doi:10.1016/j.dsro.2006.01.028.
- Coale, K. H., et al. (2004), Southern Ocean iron enrichment experiment: Carbon cycling in high- and low-Si waters, *Science*, **304**(5669), 408–414, doi:10.1126/science.1089778.
- Dobson, F. W., and S. D. Smith (1988), Bulk models of solar radiation at sea, *Q. J. R. Meteorol. Soc.*, **114**, 165–182, doi:10.1256/smsqj.47908.
- Ducklow, H. W., W. Fraser, D. M. Karl, L. B. Quetin, R. M. Ross, R. C. Smith, S. E. Stammerjohn, M. Vernet, and R. M. Daniels (2006), Water-column processes in the West Antarctic Peninsula and the Ross Sea: Interannual variations and foodweb structure, *Deep Sea Res. Part II*, **53**(8–10), 834–852, doi:10.1016/j.dsro.2006.02.009.
- Eppley, R. W. (1972), Temperature and phytoplankton growth in the sea, *Fish. Bull.*, **70**, 1063–1085.
- Fennel, K., M. R. Abbott, Y. H. Spitz, J. G. Richman, and D. M. Nelson (2003), Impacts of iron control on phytoplankton production in the modern and glacial Southern Ocean, *Deep Sea Res. Part II*, **50**(3–4), 833–851, doi:10.1016/S0967-0645(02)00596-9.
- Fitch, D. T., and J. K. Moore (2007), Wind speed influence on phytoplankton bloom dynamics in the Southern Ocean Marginal Ice Zone, *J. Geophys. Res.*, **112**(C8), C08006, doi:10.1029/2006JC004061.
- Gabric, A. J., R. Cropp, G. P. Ayers, G. McTainsh, and R. Braddock (2002), Coupling between cycles of phytoplankton biomass and aerosol optical depth as derived from SeaWiFS time series in the Subantarctic Southern Ocean, *Geophys. Res. Lett.*, **29**(7), 1112, doi:10.1029/2001GL013545.
- Garcia, C. A. E., V. M. T. Garcia, and C. R. McClain (2005), Evaluation of SeaWiFS chlorophyll algorithms in the Southwestern Atlantic and Southern Oceans, *Remote Sens. Environ.*, **95**(1), 125–137, doi:10.1016/j.rse.2004.12.006.
- Gervais, F., U. Riebesell, and M. Y. Gorbunov (2002), Changes in primary productivity and chlorophyll *a* in response to iron fertilization in the Southern Polar Frontal Zone, *Limnol. Oceanogr.*, **47**(5), 1324–1335.
- Gregg, W. W., and K. L. Carder (1990), A simple spectral solar irradiance model for cloudless maritime atmospheres, *Limnol. Oceanogr.*, **35**, 1657–1675.
- Hense, I., U. V. Bathmann, and R. Timmermann (2000), Plankton dynamics in frontal systems of the Southern Ocean, *J. Mar. Syst.*, **27**(1–3), 235–252, doi:10.1016/S0924-7963(00)00070-1.
- Holm-Hansen, O., et al. (2004), Temporal and spatial distribution of chlorophyll-*a* in surface waters of the Scotia Sea as determined by both shipboard measurements and satellite data, *Deep Sea Res. Part II*, **51**(12–13), 1323–1331.
- Kalnay, E., et al. (1996), The NCEP/NCAR 40-year reanalysis project, *Bull. Am. Meteorol. Soc.*, **77**(3), 437–471, doi:10.1175/1520-0477(1996)077<0437:TNY>2.0.CO;2.
- Korb, R. E., and M. Whitehouse (2004), Contrasting primary production regimes around South Georgia, Southern Ocean: Large blooms versus high nutrient, low chlorophyll waters, *Deep Sea Res. Part I*, **51**(5), 721–738, doi:10.1016/j.dsro.2004.02.006.
- Korb, R. E., M. J. Whitehouse, and P. Ward (2004), SeaWiFS in the Southern Ocean: Spatial and temporal variability in phytoplankton biomass around South Georgia, *Deep Sea Res. Part II*, **51**(1–3), 99–116, doi:10.1016/j.dsro.2003.04.002.
- Lancelot, C., C. Veth, and S. Mathot (1991), Modelling ice-edge phytoplankton bloom in the Scotia-Weddell sea sector of the Southern Ocean during spring 1998, *J. Mar. Syst.*, **2**, 333–346, doi:10.1016/0924-7963(91)90040-2.
- Le Quéré, C., et al. (2007), Saturation of the Southern Ocean CO₂ sink due to recent climate change, *Science*, **316**(5832), 1735–1738, doi:10.1126/science.1136188.
- Lomas, M. W., and N. R. Bates (2004), Potential controls on interannual partitioning of organic carbon during the winter/spring phytoplankton bloom at the Bermuda Atlantic Time-series Study (BATS) site, *Deep Sea Res. Part I*, **51**(11), 1619–1636.
- Lo Monaco, C., N. Metzl, A. Poisson, C. Brunet, and B. Schauer (2005), Anthropogenic CO₂ in the Southern Ocean: Distribution and inventory at the Indian-Atlantic boundary (World Ocean Circulation Experiment line 16), *J. Geophys. Res.*, **110**, C06010, doi:10.1029/2004JC002643.

- Longhurst, A., S. Sathyendranath, T. Platt, and C. Caverhill (1995), An estimate of global primary production in the ocean from satellite radiometer data, *J. Plankton Res.*, 17, 1245–1271, doi:10.1093/plankt/17.6.1245.
- Louanchi, F., M. Hoppema, D. C. E. Bakker, A. Poisson, M. H. C. Stoll, H. J. W. De Baar, B. Schauer, D. P. Ruiz-Pino, and D. Wolf-Gladrow (1999a), Modelled and observed sea surface fCO₂ in the Southern Ocean: A comparative study, *Tellus Ser. B*, 51(2), 541–559, doi:10.1034/j.1600-0889.1999.00029.x.
- Louanchi, F., D. P. Ruiz-Pino, and A. Poisson (1999b), Temporal variations of mixed-layer oceanic CO₂ at JGOFS-KERFIX time-series station: Physical versus biogeochemical processes, *J. Mar. Res.*, 57(1), 165–187, doi:10.1357/002224099765038607.
- Lovenduski, N. S., and N. Gruber (2005), Impact of the Southern Annular Mode on Southern Ocean circulation and biology, *Geophys. Res. Lett.*, 32(11), L11603, doi:10.1029/2005GL022727.
- Markus, T. (1999), Results from an ECMWF-SSM/I forced mixed layer model of the Southern Ocean, *J. Geophys. Res.*, 104, 15,603–15,620, doi:10.1029/1999JC900080.
- Markus, T., and B. A. Burns (1995), A method to estimate subpixel-scale coastal polynyas with satellite passive microwave data, *J. Geophys. Res.*, 100, 4473–4487, doi:10.1029/94JC02278.
- Marrari, M., C. M. Hu, and K. Daly (2006), Validation of SeaWiFS chlorophyll *a* concentrations in the Southern Ocean: A revisit, *Remote Sens. Environ.*, 105(4), 367–375, doi:10.1016/j.rse.2006.07.008.
- Martin, J. H. (1990), Glacial-interglacial CO₂ change: The iron hypothesis, *Paleoceanography*, 5, 1–13, doi:10.1029/PA0051001p00001.
- McClain, C. R., K. R. Arrigo, K.-S. Tai, and D. Turk (1996), Observations and simulations of physical and biological processes at OWS P, 1951–1980, *J. Geophys. Res.*, 101, 3697–3713, doi:10.1029/95JC03052.
- McNeil, B. I., B. Tilbrook, and R. J. Matear (2001), Accumulation and uptake of anthropogenic CO₂ in the Southern Ocean, south of Australia between 1968 and 1996, *J. Geophys. Res.*, 106(C12), 31,431–31,445, doi:10.1029/2000JC000331.
- Meehl, G. A., W. D. Collins, B. A. Boville, J. T. Kiehl, T. M. L. Wigley, and J. M. Arblaster (2000), Response of the NCAR climate system model to increased CO₂ and the role of physical processes, *J. Clim.*, 13(11), 1879–1898, doi:10.1175/1520-0442(2000)013<1879:ROTNC>2.0.CO;2.
- Mitchell, B. G., and O. Holm-Hansen (1991), Bio-optical properties of Antarctic Peninsula waters: Differentiation from temperate ocean models, *Deep Sea Res. Part A*, 38, 1009–1028, doi:10.1016/0198-0149(91)90094-V.
- Moore, J. K., and M. R. Abbott (2000), Phytoplankton chlorophyll distributions and primary production in the Southern Ocean, *J. Geophys. Res.*, 105(C12), 28,709–28,722, doi:10.1029/1999JC000043.
- Morel, A. (1978), Available, usable, and stored radiant energy in relation to marine photosynthesis, *Deep Sea Res.*, 25, 673–688, doi:10.1016/0146-6291(78)90623-9.
- O'Reilly, J., S. Maritorena, B. G. Mitchell, D. A. Siegel, K. L. Carder, M. Kahru, S. A. Garver, and C. R. McClain (1998), Ocean color algorithms for SeaWiFS, *J. Geophys. Res.*, 103, 24,937–24,953, doi:10.1029/98JC02160.
- Pabi, S., G. L. van Dijken, and K. R. Arrigo (2008), Primary production in the Arctic Ocean, 1998–2006, *J. Geophys. Res.*, 113, C08005, doi:10.1029/2007JC004578.
- Pope, R. M., and E. S. Fry (1997), Absorption spectrum (380–700 nm) of pure water. Part II. Integrating cavity measurements, *Appl. Opt.*, 36, 8710–8723, doi:10.1364/AO.36.008710.
- Reuer, M. K., B. A. Barnett, M. L. Bender, P. G. Falkowski, and M. B. Hendriks (2007), New estimates of Southern Ocean biological production rates from O₂/Ar ratios and the triple isotope composition of O₂, *Deep Sea Res. Part I*, 54, 951–974, doi:10.1016/j.dsri.2007.02.007.
- Reynolds, R. W., N. A. Rayner, T. M. Smith, D. C. Stokes, and W. Wang (2002), An improved in situ and satellite SST analysis for climate, *J. Clim.*, 15, 1609–1625, doi:10.1175/1520-0442(2002)015<1609:AIISAS>2.0.CO;2.
- Rind, D., R. Healy, C. Parkinson, and D. Martinson (1997), The role of sea ice in 2xCO₂ climate model sensitivity: 2. Hemispheric dependencies, *Geophys. Res. Lett.*, 24(12), 1491–1494, doi:10.1029/97GL01433.
- Russell, J. L., R. J. Souffer, and K. W. Dixon (2006a), Intercomparison of the Southern Ocean circulations in the IPCC Coupled Model Control Simulations, *J. Clim.*, 19(18), 4560–4575, doi:10.1175/JCLI3869.1.
- Russell, J. L., K. W. Dixon, A. Gnanadesikan, R. J. Stouffer, and J. R. Toggweiler (2006b), The Southern Hemisphere westerlies in a warming world: Proposing open the door to the deep ocean, *J. Clim.*, 19(24), 6382–6390, doi:10.1175/JCLI3984.1.
- Sabine, C. L., R. A. Feely, R. M. Key, J. L. Bullister, F. J. Millero, K. Lee, T. H. Peng, B. Tilbrook, T. Ono, and C. S. Wong (2002), Distribution of anthropogenic CO₂ in the Pacific Ocean, *Global Biogeochem. Cycles*, 16(4), 1083, doi:10.1029/2001GB001639.
- Sarmiento, J. L., T. M. C. Hughes, R. J. Stouffer, and S. Manabe (1998), Simulated response of the ocean carbon cycle to anthropogenic climate warming, *Nature*, 393, 245–249, doi:10.1038/30455.
- Sarmiento, J. L., N. Gruber, M. A. Brzezinski, and J. P. Dunne (2004), High-latitude controls of thermocline nutrients and low latitude biological productivity, *Nature*, 427, 56–60, doi:10.1038/nature02127.
- Skogen, M. D., and A. Moll (2000), Interannual variability of the North Sea primary production: Comparison from two model studies, *Cont. Shelf Res.*, 20(2), 129–151, doi:10.1016/S0278-4343(99)00069-2.
- Smith, R. C., and K. S. Baker (1981), Optical properties of the clearest natural waters (200–800 nm), *Appl. Opt.*, 20(2), 177–184.
- Smith, W. O., Jr., and L. I. Gordon (1997), Hyperproductivity of the Ross Sea (Antarctica) polynya during austral spring, *Geophys. Res. Lett.*, 24, 233–236, doi:10.1029/96GL03926.
- Smith, W. O., Jr., and D. M. Nelson (1986), Importance of ice-edge phytoplankton production in the Southern Ocean, *BioScience*, 36, 251–256, doi:10.2307/1310215.
- Steinberg, D. K., C. A. Carlson, N. R. Bates, R. J. Johnson, A. F. Michaels, and A. H. Knap (2001), Overview of the US JGOFS Bermuda Atlantic Time-series Study (BATS): A decade-scale look at ocean biology and biogeochemistry, *Deep Sea Res. Part II*, 48, 1405–1447, doi:10.1016/S0967-0645(00)00148-X.
- Sullivan, C. W., K. R. Arrigo, C. R. McClain, J. C. Comiso, and J. Firestone (1993), Distributions of phytoplankton blooms in the Southern Ocean, *Science*, 262, 1832–1837, doi:10.1126/science.262.5141.1832.
- Sweeney, C. (2003), The annual cycle of surface water CO₂ and O₂ in the Ross Sea: A model for gas exchange on the continental shelves of Antarctica, in *Biogeochemistry of the Ross Sea*, Ant. Res. Ser., vol. 78, edited by R. Dunbar and G. DiTullio, pp. 295–312, AGU, Washington, D. C.
- Takahashi, T., et al. (2002), Global sea-air CO₂ flux based on climatological surface ocean pCO₂, and seasonal biological and temperature effects, *Deep Sea Res. Part II*, 49(9–10), 1601–1622, doi:10.1016/S0967-0645(02)00003-6.
- Thompson, D. W. J., and S. Solomon (2002), Interpretation of recent Southern Hemisphere climate change, *Science*, 296, 895–899, doi:10.1126/science.1069270.
- Turner, J., J. E. Overland, and J. E. Walsh (2007), An Arctic and Antarctic perspective on recent climate change, *Int. J. Climatol.*, 27(3), 277–293, doi:10.1002/joc.1406.
- Waugh, D. W., T. M. Hall, B. I. McNeil, R. Key, and R. J. Matear (2006), Anthropogenic CO₂ in the oceans estimated using transit time distributions, *Tellus Ser. B*, 58(5), 376–389, doi:10.1111/j.1600-0889.2006.00222.x.

K. R. Arrigo, S. Bushinsky, and G. L. van Dijken, Department of Environmental Earth System Science, Stanford University, Stanford, CA 94305, USA. (arrigo@stanford.edu)